Stereotactic Body Radiation Therapy

13

Steven J. Feigenberg, Randi Cohen, Navesh K. Sharma, Zain Husain, Shifeng Chen, and Laura A. Dawson

Introduction

Over the last 30 years, advances in immobilization, computer-based treatment planning and delivery, and image guidance have revolutionized the ways in which small tumors are treated with radiation therapy (RT). Stereotactic radiosurgery (SRS) was introduced in 1968 as a tool for noninvasive neurosurgery but was not widely adopted until three-dimensional imaging became available. The pinpoint accuracy and high-dose concentration achievable with SRS have allowed high "tumor ablative" treatment of target tissues. SRS has been a success story for patients with brain metastases by improving local control, quality of life, and survival. Its success has hinged on minimizing the volume of normal tissue receiving a "significant" dose of radiation while maximizing dose to the tumor.

SRS outside the brain, called stereotactic body RT (SBRT) or more recently stereotactic radioablation (SABR), has been more challenging. Treatment planning of intracranial targets involves delivery of a very conformal dose of radiation to the radiographic target with no margin, because the brain does not move in reference to the rigid stereotactic head frame. When the target is located outside the brain, immobilization is less accurate and organ/tumor motion requires the physician to add a margin to account for these differences to ensure appropriate dose to the gross target volume (GTV). The planning target volume (PTV) is defined by an additional margin to account for tumor motion and setup uncertainties. This added margin increases the volume of tissue irradiated, which theoretically increases the risk of side effects. Over the last 15 years, solutions have allowed SBRT/SABR to treat tumors outside the brain.

SBRT refers to the use of a limited number of high-dose fractions delivered conformally to targets with high accuracy, using biologic doses of radiation far higher than those used in standard fractionation. *Stereotactic* refers to the use of a reference system to aid in localizing the tumor. An external reference system, such as a stereotactic head frame for cranial SRS or internal fiducial markers including the tumor itself, may be used for localization and guidance. For tumors fixed to bony anatomy, such as base of skull cancers, image guidance using bony anatomy may be appropriate; however, often the position of the tumor is not highly correlated with the bones or an external reference system, and imaging and targeting of the tumor itself (i.e., image-guided radiation therapy [IGRT]) may be required.

SBRT is becoming more popular, as evidenced by increasing recognition at international meetings, a textbook devoted to the topic [1], and an American Society for Therapeutic Radiology and Oncology (ASTRO) consensus document on SBRT [2]. The ASTRO consensus document defines SBRT as high-precision radiotherapy delivered in three or more fractions to very potent doses of highly conformal radiation with steep dose gradients around the target. SBRT is "an evolving technology," and definitions may change with time. The philosophies and techniques of SBRT can be applied to longer fractionation regimens (when the target is intimately associated with a critical serial functioning normal tissue, for example) or shorter fractionations, including SRS.

Similar to cranial SRS, multiple static or dynamic beams in a variety of beam arrangements, with or without segments or intensity modulation, can be used to produce a dose distribution in which isodose lines tightly conform to the target volume. Although most reports on SBRT refer to megavoltage photon irradiation, protons are not excluded from the SBRT definition. Inhomogeneity within the target volume is

S.J. Feigenberg, M.D. (✉) • R. Cohen, M.D., M.S. • N.K. Sharma, D.O., Ph.D. • S. Chen, Ph.D.
Department of Radiation Oncology, The University of Maryland School of Medicine, Baltimore, MD, USA
e-mail: sfeigenberg@umm.edu

Z. Husain, M.D.
Department of Therapeutic Radiology, Yale University, New Haven, CT, USA

L.A. Dawson, M.D., F.R.C.P.C.
Department of Radiation Oncology, Princess Margaret Cancer Centre, University of Toronto, Toronto, ON, Canada

L.S. Chin and W.F. Regine (eds.), *Principles and Practice of Stereotactic Radiosurgery*,
DOI 10.1007/978-1-4614-8363-2_13,

permitted and hot spots have been encouraged within the PTV to increase the chance of tumor ablation, although with a larger rim of normal tissue found inside of the target volume in comparison to cranial SRS that complications may be increased. Dose is generally prescribed to an isodose line covering the PTV similar to cranial SRS, with a very steep dose gradient outside the PTV.

SBRT is a noninvasive, outpatient intervention, generally completed within 1 or 2 weeks, allowing for little to no delays in systemic therapy. The short radiation treatment time and high dose per fraction in SBRT have potential radiobiological therapeutic advantages compared with conventional fractionation, due to less tumor repopulation and repair. In addition, there is growing evidence that SBRT/SABR may have an impact on disease outside of the treated volume decreasing regional and distant recurrences, the "abscopal effect." Furthermore, the shorter SBRT treatment times are more convenient for patients and have resource utilization advantages.

The rationale for SBRT is that there is a need for improved local therapies for many primary cancers and also in the situation when there are "oligo" (i.e., isolated) metastases, specifically in sites where surgery has been shown previously to be able to cure patients with "oligo" metastases (e.g., colorectal cancer (CRC), renal cell cancer, and sarcoma). SBRT is less invasive than surgery, and once the safety of SBRT has been established, SBRT has the potential to be used in place of surgery in situations when surgery may be associated with high risk. Even in incurable situations, SBRT may be of significant advantage to patients with metastatic disease on systemic therapy where only a few tumors are increasing in size and the rest of their disease is stable. Patients could be maintained on their current systemic therapy, if they are tolerating, rather just changing to a new systemic therapy of unknown efficacy and morbidity potentially improving quality of life.

In this chapter, a historical perspective, rationale, technical details, and literature on SBRT/SABR outcomes and complications will be reviewed. Specific applications of SBRT will be reviewed in more detail where there is an abundance of data including lung cancer and metastases, liver metastases and hepatocellular carcinoma (HCC), spinal malignancies and pancreatic cancer.

Historical Perspective

The first extracranial site to be investigated with SRS techniques was the spine in 1993. A rigid skeletal fixation device that immobilized the spine above and below the target was used as a stereotactic reference frame to guide radiation [3]. Around the same time, Blomgren and Lax [4, 5] from Sweden began applying stereotactic techniques to body targets such as lung and liver tumors. They developed a body stereotactic reference frame to aid in guidance of radiation. Blomgren et al. [5] reported their initial experience in 1995, in which 31 patients with primarily solitary lung and liver tumors were treated with one to four fractions. Reproducibility of this approach, based on patients who had repeat CT scans in the treatment position, was found to be within 5 (axial) to 8 (cranial–caudal) mm for 90 % of setups with diaphragm motion reduced to 5–10 mm with abdominal pressure.

Experience in North America has been growing exponentially following the pioneering work of Dr. Timmerman [6–9] who systematically evaluated SBRT by a series of prospective clinical studies. Based on this experience, he led the Radiation Oncology Therapy Group (RTOG) initiative with a multi-institutional phase II trial of SBRT in lung cancer which was published in 2010 in JAMA [10]. The results were so impressive that the paradigm of surgery as the standard of care for small tumors is currently being challenged in RTOG 10–14 [11]. Similar North American studies have been reported for liver metastases, vertebral metastases, adrenal metastases, pancreatic carcinomas, recurrent head and neck cancers as well as for tumors of the retroperitoneum and pelvis.

Radiobiology

Radiobiologic Models

The linear quadratic model may not be valid for very short fractionation schemes. In the early development of this model, one of the developers expressed that the model is not intended for doses higher than 8–10 Gy. The linear quadratic model may overpredict tumor cell kill and underpredict toxicity at the increased dose per fraction. Fowler et al. [12–14] predicted that local control should be excellent for non-small cell lung cancer (NSCLC) with biological doses of the order 100 Gy in 2-Gy equivalent dose or higher ($\alpha/\beta = 10$), although based on the pioneering work at Michigan [15, 16] the local control was only 70 % at this dose level. Although there seems to be a threshold of superior local control at 100 Gy ($\alpha/\beta = 10$) when higher doses per fraction are used. Fractionation schemes with an estimated tumor control probability (TCP) of 95 % or greater include 45 to 60 Gy in three fractions and 60 Gy in five fractions, although one must be extremely careful to review how the dose was prescribed as investigators prescribe dose very differently. German investigators [17] prescribe dose to the 65 % isodose shell while the Japanese routinely prescribe to the isocenter—which can lead to very different doses seen by the PTV. Due to the inadequacies in the linear quadratic model in predicting outcomes, investigators [18] have developed the universal survival curve. This combines the linear quadratic model and the multi-target model which may be more accurate. Although as the investigators correctly point out, "the complex biology

that underlies cell ablation and loss of clonogenicity precludes an explanation by any simple mathematical model."

Mechanism of Action

It is clear that the mechanism of cell kill is different between a conventionally fractionated course of radiotherapy as opposed to the "ablative" doses used with SBRT. The classic model of radiobiology is defined by the depletion of tumor stem cells and undifferentiated progenitor clonogens for radiotherapy to be curative. With conventionally fractionated radiotherapy where large volumes of normal tissue receive the prescribed treatment dose, normal tissue stem cells are better at repairing radiation damage than tumor clonogens. The surrounding microenviroment was not thought to be an active contributor to this effect until recently. As a possible explanation, Fuks et al. [19] initially suggested that contrary to conventional (1.8–3 Gy) fractionation, high-dose radiation (>8–10 Gy per fraction) specifically impacts more robust endothelial apoptosis and microvascular dysfunction, which in turn leads to increased cell death. Furthermore, hypoxia resulting from standard fractionated radiotherapy regimens results in a burst of pro-angiogenic activity in the tumor microenvironment, generating HIF-1α, VEGF, and other vasculogenic factors which, in turn attenuate radiation-induced apoptosis in endothelial cells.

Immune Response to Radiation

SBRT appears to impact disease outside the radiated volume. This is best exemplified by a retrospective experience from William Beaumont Hospital [20] which compared patients who were treated with either a sublobar resection or SABR during the same time period. SABR not only resulted in a drastically lower local failure rate (5 % versus 24 %, $p=0.05$), but more unexpectedly had a lower regional lymph node failure rate (18 % versus 0 %, $p<0.05$) even though patients were more likely to be surgically staged to be node negative in the resected cohort (71 % versus 20 %). Given that patients treated using SABR have a very small (tumor plus margin) volume of tissue irradiated, and few if any lymph nodes included in the treatment field, this was a surprising finding. One possible explanation of this phenomenon is the stimulation of T-cell immunity by SABR, leading to the eradication of occult regional micrometastases.

The immune system has long been known to play a critical role in tumor surveillance and control [21]. It is thought that tumors develop by escaping immune detection, either by downregulating surface recognition antigens or by releasing immunomodulatory cytokines that dampen the immune response, and are found in greater prevalence in immunosuppressed populations. Conversely, a robust immune response, associated with cytotoxic immune cell populations, is associated with improved tumor control [22]. Radiotherapy, in its classic delivery with standard fractionation, has traditionally been viewed as an immunosuppressive modality [23]. However, the actual effects on the immune system are extremely complex with conflicting reports on whether they promote or interfere with tumor reduction.

One of the leading hypotheses for this "abscopal" effect with SBRT is its relationship to $CD8^+$ T-cell-mediated immune response. The lower than expected regional failure rate with SBRT may be due to radiation-induced systemic stimulation of T-cell immune responses, leading to eradication of occult regional micrometastases. Support for this theory derives primarily from experiments in animal models. A recent study examined the effect of ablative doses of radiation therapy in a mouse melanoma model [24]. In this study, mice with B16 melanoma tumors received 20 Gy of radiation in a single fraction. Examination of the tumor microenvironment and lymphoid tissues 1–2 weeks posttreatment demonstrated tumor regression and an increase of infiltrating T cells. When the experiment was repeated with athymic nude mice, which lack T cells, no statistically significant decrease in tumor volume was observed, suggesting that the effects were T-cell mediated. Taken together, these studies suggest that ablative doses of radiation alter the tumor microenvironment, causing T-cell infiltration resulting in vigorous priming and expansion of effector T cells. The experiment was repeated in wild-type mice with B16 tumors, which had been subjected to antibody-mediated $CD8^+$ T-cell depletion. The therapeutic benefit to the ablative radiation was diminished, and survival in this $CD8^+$ depleted group was decreased by 75 %. In a separate experiment using a transplantable mouse 4T1 mammary carcinoma model (which mimics metastatic ability of breast cancer cells to lung, bone, liver, etc.), ablative radiation therapy delivered to the primary tumor site led to a complete elimination of lung metastasis. This observation strongly suggests the induction of a potent antitumor immune response. Separate experiments utilizing CD8 depletion strategies demonstrate a relative increase in number of distant metastases, again suggesting that $CD8^+$ T cells are critical for mediating protection against tumors. Taken in combination, these studies suggest that $CD8^+$ T cells play a critical role in radiation-induced antitumor immune responses (both locally and distantly), following ablative dose therapy.

Clinically, similarly suggestive observations have been reported in several tumor types. Mahmoud et al. [25, 26] recently demonstrated the influence of density and distribution of the cytotoxic $CD8^+$ T cells in breast cancer patients. Using immunohistochemistry staining of tissue microarray cores, they established that infiltration of $CD8^+$ T cells into the distant stroma correlated with improved overall survival. In addition, the number of T regulatory cells, the ratio of $CD4^+$ to $CD8^+$ T cells, and the presence of T lymphocytes in the primary tumor correlated with grade, stage, and survival.

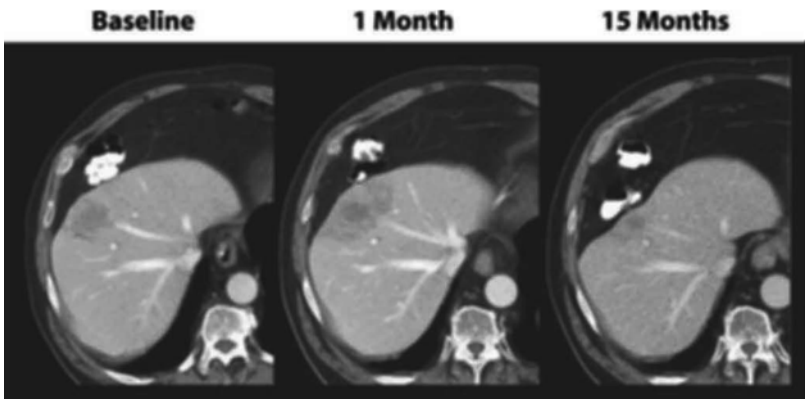

Fig. 13.1 Baseline CT of isolated liver metastases and follow-up imaging at 3 months and 18 months revealing no evidence of progressive disease

Furthermore, several groups have demonstrated that the presence of tumor-associated lymphocytes in breast cancer is an independent predictor of response to anthracycline/taxane-based chemotherapy [27]. Paulson et al. [28] have demonstrated that intratumoral $CD8^+$ lymphocyte infiltration was the most important predictor of outcomes in patients with Merkel cell carcinoma. Interestingly, in this population, patients with tumors that demonstrated a robust $CD8^+$ lymphocyte infiltration were observed to have the largest improvements in regional and distant control as compared to local control. A recently published report [29] appears to substantiate this combination of ipilimumab with SABR. In this case study, a patient with progressive metastatic melanoma receiving maintenance ipilimumab therapy was treated palliatively with SABR for a painful paraspinal mass. While there was no initial response, a single additional dose of ipilimumab not only significantly decreased the size of the paraspinal mass but also caused regression of additional sites of metastatic disease which were of considerable distance from the radiated paraspinal mass. Further analysis demonstrated that RT had increased antibodies to NY-ESO-1, an antigen associated with melanoma, by 30-fold. Since presence of antibodies to NY-ESO-1 had been associated with a more robust response to ipilimumab, this may explain why this patient had such an excellent response to disease within and outside the radiation portal. Furthermore, the RT regimen in this patient also led to a subsequent spike in inducible co-stimulator, a marker of activated CTLs, suggesting an additional mechanism for the observed tumor control.

Imaging Response to SBRT

With these promising early results, two cooperative groups are evaluating SBRT as an alternative to surgery. However, assessment of tumor response to SBRT in a time frame that will allow those with failures the maximal curative benefit from salvage surgery remains a challenge. Furthermore, in the medically inoperable population, identifying the extent of tumor response to initial SBRT is critical in determining further treatment response, as is identifying dose–response characteristics on current SBRT trials. Specifically, is there an imaging technique that can be used as a biomarker or early surrogate marker of outcome? Currently, computerized tomography remains the imaging modality of choice to evaluate response following SBRT. However, with the very high-dose fractions utilized in SBRT, a significant percentage of patients treated by SBRT will develop fibrosis within and in close proximity to the treatment field. Takeda et al. [30, 31] described solid consolidations on CT scans are seen as late changes in the center or the periphery of the PTV in upwards of 73 % of patients. Radiographic findings, that occur as a result of SBRT, are more dramatic in appearance as opposed to what is seen clinically (see Fig. 13.1). These consolidations can be quite complex making serial CT follow-up rather difficult, thereby making it difficult to determine whether these changes are consistent with recurrent carcinoma or radiation changes.

In this regard, assessment of tumor response to therapy using functional information could be very helpful in the absence of good anatomical imaging such as 18-fluorodeoxyglucose-positron emission tomography (FDG-PET) scanning modality. PET scans have had a significant impact on the management of patients with many cancers but it has been studied most extensively in NSCLC. Their most important contribution has been in the improvement in the preoperative evaluation of mediastinal lymph nodes over computed tomography (CT) scans alone with increased sensitivity and specificity [32–34] and in staging improving patient selection for curative therapy. FDG-PET has also been prognostic in the pretreatment setting and following induction chemotherapy [35] or definitive chemoradiotherapy to determine tumor response as defined by FDG uptake for predicting outcomes [36, 37]. Following SBRT, PET findings have been mixed with only a few small series reported.

A small prospective series [38] from Fox Chase Cancer Center which included ten medically inoperable patients treated for NSCLC on a phase I dose escalation demonstrated that a drop in the maximum standardized uptake values (SUV) comparing the pre-SBRT and the 3-month post-SBRT PET scan appeared to be a predictor of local control. A larger retrospective experience [39] from the same institution including 26 patients addressed using FDG-PET response (comparing pre-SBRT versus 3-month post-SBRT) as a surrogate of local failure in greater detail. All 26 PET scans were reviewed and interpreted by a single physician who was blinded to the clinical results. FDG-PET scans were analyzed semi-quantitatively by comparing pre- and post-treatment changes in SUV. This study demonstrated two major findings: (1) A lower initial SUV value was the only significant factor associated with an increased risk of local failure (3.4 versus 5.7; $p=0.045$) with 4 out of the 5 local failures having a low pre-SBRT SUV (<4). (2) Decreases in post-SBRT SUV of >55 % of its pre-SBRT value significantly decreased the risk of local recurrence. Similar findings were seen when this data was combined with data from the University of Maryland [40] which demonstrated a crude local failure rate of 54.5 % failure rate (6/11) for patients with SUV <4, while only 11 % (4/36) of patients with SUV ≥4 failed locally. Hoopes et al. [41] have described with nearly 50 % of patients at 1 year having SUVmax changes >3.5 from their prospective study and 15 % in their retrospective experience (4 of 28 with a max SUV >2.5). Presumably, though, all were lower than pretreatment. These patients were too compromised to undergo further treatment and were thus followed. They remained without recurrence between 8 and 22 months post these PET scans. This illustrates that the use of a specific SUV value is not useful and therefore trying to determine a specific cutoff SUV for a population to predict recurrence is not appropriate. With these inflammatory changes so prevalent, it is imperative for the reading nuclear medicine physician and treating physician to review the images to define the solid and inflammatory components and their corresponding SUV in relationship to the distribution of the treatment to minimize the possibility of false-positive readings. It is therefore to our advantage to have scans read by a single physician for consistency in reporting.

Further refinement of this data is vital as quantification with SUVmax oversimplifies the evaluation of tumor response and sometimes results in inconclusive or inaccurate diagnosis. Currently investigators are trying to extract more detailed spatial–temporal PET/CT features [42] that comprehensively characterize the whole tumor's intensities and distributions, spatial variations (texture), and shape properties which may become better predictors of treatment response. In addition, novel radiotracers are in development. The use of fluorodeoxyglucose (FDG) as the radiotracer of choice for PET scanning has been recently challenged. Investigators have looked at L-*s*-methyl-11C methionine (MET) PET. While MET has been shown to have decreased in inflammatory lesions as compared to FDG, a small series from Japan in the SBRT setting showed very little difference between the two tracers [43]. ^{18}F -3′-fluoro-3′-deoxy-L-thymidine (FLT) [44], a nucleoside reverse transcriptase inhibitor, has been suggested to be superior to that of FDG in detecting cellular and proliferative responses to chemotherapy; the role of FLT-PET as a surrogate of response following stereotactic body radiotherapy (SBRT) for lung cancer remains unexplored. Similar data is available for patients with liver metastases and lung metastases.

Normal Tissue Response to SBRT

Normal tissues that function primarily as parallel normal tissues are made up of predominately structurally defined functional subunits (FSUs) (e.g., peripheral lung, liver, kidney). Serial functioning normal tissues, characterized by a chain of function, are composed of primarily undefined FSUs (e.g., gastrointestinal mucosa, trachea, spinal cord, bronchus). Parallel organ toxicity is mostly related to volume irradiated (e.g., mean dose, volume treated to a threshold dose such as V20), whereas serial organ toxicity is mostly related to the maximum dose delivered to that tissue. Although useful, this distinction between serial and parallel functioning organs is likely too simplistic, and most normal tissues likely have both parallel and serial functionality. This has been demonstrated in elegant rat model experiments of spinal cord tolerance to radiation therapy by van der Kogel et al. [45]. The rat spinal cord tolerance to radiation was found to be dependent on the volume irradiated and the spatial distribution of dose. The gray matter of the cord was found to be most resistant, whereas the lateral white matter was most sensitive.

As the volume of normal tissues irradiated to high doses with SBRT is generally less than the volume of normal tissue irradiated with conventional fractionation, for normal tissues that are primarily parallel functioning, if the volume irradiated is low enough, the risk of toxicity may be extremely low despite delivery of very high doses to a small volume. However, for serial organs that are in close proximity to tumors, even a small volume irradiated to a high dose may lead to irreversible toxicity. Thus, SBRT should be used cautiously for tumors adjacent to serial functioning organs such as the esophagus or spinal cord. An increase in the number of fractions may improve the therapeutic ratio and should be considered in place of hypofractionated SBRT in this situation.

With a dramatic increase in the fraction size and total dose with SBRT, the repair mechanisms may not be initiated as they would at a lower dose per fraction, potentially leading to permanent damage to the normal tissue within the

high-dose volumes and/or unpredictable effects outside the high-dose volume. Given the potential for normal tissue injury and that the volume tolerance of normal tissues to such high doses per fraction is unknown, most SBRT has been applied to small tumors (<5 cm) in which the volume of normal tissue around the tumor is small. SBRT is being investigated for larger tumor volumes [46], and it is hopeful that clinical data will eventually be obtained to provide guidance to what the dose–volume toxicity relationship is for organs irradiated with inhomogeneous doses from hypofractionated fractionation schemes.

As very steep dose gradients are used with SBRT with rapid falloff of dose in surrounding normal tissues, not only is there substantial variability of dose throughout normal tissues, but also there is substantial variability in the dose per fraction. Thus, when dose–volume characteristics of a normal tissue associated with toxicity risk are investigated, correction for the variability in dose per fraction should be considered. Unfortunately, accurate knowledge of the α/β ratio for normal tissues is lacking. Clinical trials of novel fractionation regimens are required to confirm outcomes and toxicities associated with the many different fractionation schemes used in SBRT. Under each of the clinical sections, additional data will be presented based on complications to the bowel, chest wall, rib, liver, and brachial plexus.

Immobilization

Overview

Given the sensitivity of highly conformal SBRT plans to setup uncertainty and organ motion, reduction of geometric uncertainties and organ motion is important. The choice of patient position and immobilization may impact setup error, organ motion, as well as intrafraction motion secondary to patient discomfort. For example, prostate motion due to breathing is reduced in the supine position compared with the prone position [47, 48]. The different immobilization devices and strategies that have been used for SBRT are described below.

Spinal Tumor Immobilization

Similar to intracranial SRS with a cranial halo secured to the skull with transcutaneous pins, rigid fixation systems have been used for paraspinal and spinal SBRT. Hamilton in 1995 immobilized the spine for SBRT with rigid skeletal fixation above and below the involved segments. With this system, excellent accuracy, with less than 2-mm offsets, was observed [3]. However, such an approach is invasive, and avoidance of invasive fixation systems is desirable to minimize risks.

Noninvasive stereotactic systems using a frame, with or without implanted fiducial markers, have been used for paraspinal tumor SBRT with accuracy within 2 mm [49]. Optical-guided three-dimensional ultrasound has also been used for spinal SBRT to ensure that the patient does not move during radiation [50].

Body Tumor Immobilization

Nonrigid fixation has been performed for SBRT with specialized body frames that have fiducial systems attached to the frame and a device to control respiration using abdominal compression [4]. Abdominal compression using such frames has been found to reduce diaphragm caudal–cranial motion to less than 5–10 mm in most patients. Reproducibility of target positioning using these frames has been reported to be better than conventional immobilization systems, with positional deviations of lung cancer and liver cancer position less than 10 mm in 98 % of patients [4, 51, 52].

An option to these specialized body frames that facilitates guidance is to not use the frames for guidance, but to image internal anatomic references, such as bones near the target or the soft tissue tumor itself, to define the treatment coordinates. Repositioning and repeat verification imaging are required to ensure the patient was moved to the correct position. A variety of immobilization devices can been used with this strategy, as long as they keep the patient immobilized and preferably are (relatively) comfortable to minimize intrafraction patient motion.

Assessment of Breathing Motion

Organ motion due to physiologic functions during a radiation treatment fraction can be substantial. For example, the liver can move up to 5 cm in the caudal–cranial direction during free breathing [53] causing motion of the upper abdominal and lower thoracic cavity. As this motion can result in alternations in target and normal organ volume definitions, PTV margins, and the entire dose distribution, interventions to reduce the impact of intrafraction organ motion are required for many SBRT patients, to facilitate dose escalation and to reduce the volume of normal tissue irradiated.

Strategies to compensate for breathing motion include the use of abdominal pressure, voluntary shallow breathing, voluntary deep inspiration, voluntary breath holds at variable phases of the respiratory cycle, active breathing control (ABC), gated radiotherapy, and real-time tumor tracking. Although voluntary breath holds may be beneficial for some patients, there is potential for leaking air and patient error, particularly for patients with lung disease where usually less than 30 % of patients can even tolerate this approach.

ABC refers to organ immobilization with breath holds that are controlled, triggered, and monitored by a caregiver. In approximately 60 % of patients with liver cancer, ABC was used successfully, with excellent reproducibility of the liver relative to the vertebral bodies within the time period of one radiation fraction (intrafraction reproducibility, σ, of the liver relative to the vertebral bodies: 1.5–2.5 mm) [54, 55]. However, with ABC, from day to day the position of the immobilized liver varies relative to the bones (interfraction reproducibility, σ 3.4–4.4 mm), providing rationale for daily image guidance when ABC is used for liver SBRT although treatment time needs to be kept reasonable as patients with poor performance status have increased treatment uncertainties and all patients have increased uncertainties with treatment times >10 min due to fatigue, muscle relaxation, or peristalsis.

Gated radiotherapy, with the beam triggered to be on only during a predetermined phase of the respiratory cycle, usually refers to the use of an external surrogate for tumor position (as opposed to direct tumor imaging) to gate the radiation. This can be used to reduce the volume of normal tissue irradiated. Changes in baseline organ position can occur from day to day [56], and thus image guidance is important to avoid geographic misses, especially in the setting of SBRT. One concern regarding gated radiotherapy has been brought to light by a French prospective phase III trial presented at ASTRO 2012 [57]. This trial was testing the benefit of gating in locally advanced lung cancer setting and surprisingly demonstrated an increase in radiation pneumonitis in patients treated with gating. The manuscript will hopefully shed more light on other variables that led to this paradoxical finding but more importantly should put caution in inexperienced users of this technology.

Tumor tracking is another approach to reduce adverse effects of organ motion. An elegant real-time tumor tracking system consisting of fluoroscopic X-ray tubes in the treatment room allowing visualization of radiopaque markers in tumors was first described by Shirato et al. The linear accelerator is triggered to irradiate only when the marker is located within the planned treatment region [58]. As an alternative to turning the radiation beam off when the tumor moves outside treatment region, multileaf collimators, the couch position, or the entire accelerator on a robotic arm may move with the tumor to ensure adequate tumor coverage at all times (e.g., CyberKnife image-guided radiosurgery system; Accuray, Sunnyvale, CA). The latter system uses dual orthogonal fluoroscopy tubes to track radiopaque markers in or near the tumor at a preset frequency.

There are advantages to gating, breath hold, and tracking in exhalation phase of the respiratory breathing cycle versus inhalation. These include the fact that exhalation tends to be more reproducible and is longer than inhalation, so that treatment during exhalation reduces duty time. However, in certain situations, there may be rationale for breath hold, gating, or tracking during inhalation. For example, for lung tumors and/or tumors adjacent to the heart, inhalation will reduce the density of the lungs and/or may move critical structures away from the target volume.

Other approaches to minimize respiratory and non-respiratory organ motion include maintaining the same preparative regimen prior to each treatment and ensuring comfortable immobilization and short overall treatment time to reduce patient movement due to discomfort and physiologic change in organs such as stomach filling. Another general intervention is patient feedback, either auditory or visual. Ideally, feedback would be from direct tumor imaging; however, feedback from imaging of adjacent organs, spirometry, nasal flow monitoring, external marker position, or optical monitoring of body contour are often more practical options. If indirect measures of organ position are used, confirmation for an individual patient that the indirect measure is indeed directly related to organ position is mandatory.

Treatment Planning

Overview

As dose gradients are steeper and doses are higher with SBRT than with conventional radiation therapy, the consequences of error in tumor delineation, errors introduced by dosimetry, and geometric uncertainties may be more deleterious. Thus, all aspects of treatment planning that are important in conformal radiation planning are even more crucial in SBRT, especially for tumors in close proximity to critical normal tissues, where a systematic error could lead to permanent serious toxicity if the normal tissue planned to be spared from radiation is irradiated to the high doses planned for the tumor.

Imaging at Simulation

At the time of simulation, patient positioning and the imaging modality (CT, MRI, PET/CT), resolution (e.g., CT thickness), and phase of contrast (e.g., arterial IV contrast for HCC or how to give IV contrast during a four-dimensional scan for a tumor near a major vessel) must be chosen carefully. The patient treatment position should be kept the same as scanning position. Due to the relatively long treatment time, a comfortable patient position is preferred to reduce the intrafraction motion. Since more beams are used at SBRT planning and they need to be separated maximally in space, beam arrangement should be considered during patient simulation. For example, for lung cancer patient, lifting both arms allows beam arrangements in 360°. The report of AAPM Task

Group 101 [59] has recommendations about the CT thickness and scanning length. In this report, 1–3-mm CT slice thickness was recommended and a typical CT scan for planning purpose should cover the tumor site plus 5–10 cm in both superior and inferior directions. If non-coplanar beams are used, 15 cm is recommended to be extended in both superior and inferior directions. Motion must be considered at this time, as breathing introduces artifacts in the tumor definition, normal tissue definition, and resultant errors in TCP and normal tissue complication probability (NTCP). Furthermore, if motion is not considered, there is potential for a systematic error from the time of simulation to the time of treatment to occur. Motion due to breathing is largest for tumors near the diaphragm (i.e., the upper abdomen and the lower thorax). One method to account for motion is to eliminate it, for example, with a breath-hold scan. Diagnostic breath-hold scans are often obtained in the inhale position, which may not correspond with the treatment position (e.g., exhale breath hold). An effort to conduct all imaging to be used for planning with the patient in the same position, with the same phase of breath hold, is required. If breath hold is not possible or if reproducibility of this breath hold cannot be documented, reduction of breathing motion may help reduce the negative impact of breathing motion. However, even with a small range of breathing motion, errors in tumor and normal tissue volumes may occur, resulting in a geographic miss or excessive toxicity. An option to breath-hold imaging is to obtain a four-dimensional imaging data set. From this, any position could be used for planning and image guidance [56]. Planning on the exhale data set with asymmetric PTV margins is an option [60], as is planning using the mean tumor position. The phase of the breathing cycle in which the patient is planned should correspond with the phase of breathing cycle used for image guidance and treatment.

Target Volumes

A decision has to be made regarding whether a margin is required for microscopic disease risk or the clinical target volume (CTV) margin. Although in many SBRT series, no extra margin for CTV has purposely been added but due to the less steep falloff in dose when treating the body as compared to the brain, there is always a dose gradient from the prescription dose to a "microscopic dose" [61]. In addition, the additional margin added for motion and setup error likely overlaps with the needed margin extension. This added margin may also be significantly different based on histology where subclinical disease distant from the index lesion is more prevalent such as in breast cancer. At Princess Margaret Hospital in Toronto, for our present SBRT liver cancer studies, a 5-mm margin around the GTV within the liver is used to define the CTV. The planned minimum dose to the CTV PTV is 27 Gy in six fractions, while the dose to the GTV may be as high as 60 Gy in six fractions at the periphery. Careful radiologic–pathologic studies accounting for organ deformation and shrinkage are required to determine whether the use of a CTV margin is required or not.

Finally, appropriate PTV margins must be used to ensure that the actual planned doses are delivered to the tumor. The PTV margins must consider setup uncertainty and internal organ motion. Individual institution setup uncertainty data should be used if available. Individual patient internal organ motion is preferable to using population-based respiratory motion. Of note, the classic PTV margin papers on PTV margin determination, such as that published by Van Herk et al. [62], do not apply to very tightly conformal plans delivered in a few fractions, such as those used in most SBRT cases. Thus, the margin recipes that are used for conventional radiation planning may be inappropriate for SBRT plans. Modeling has demonstrated that when PTV margins are too small, higher doses must be delivered for the same TCP [63].

Planning

Often, many beams or dynamic conformal arcs are used to develop a highly conformal SBRT dose distribution. In principle, a great number of beams maximumly separated in space lead to more conformal plan; however, the beam optimization should consider target size and irregularities, OAR avoidance, the length of beam path, the treatment delivery time, and patient safety. The energy of 6–10 MV is preferred due to the neutron contamination and the larger penumbra of high-energy photon beam. Limited high-energy beam may be allowed if the beam path is larger than 10 cm. Sometimes, non-coplanar beams or arcs are used if required to reduce the dose to normal tissues. For example, 8–12 beams may be used for a typical lung SBRT plan. Non-coplanar beam setup should be used carefully to avoid the patient, couch, and gantry collision. Although the more beams are preferred in SBRT planning, the resultant longer treatment time has to be considered in practice. One strategy to obtain highly steep dose gradients at the edge of the PTV is to close the aperture of the beams to the PTV or less, not leaving a gap for penumbra as usually done for conformal radiation therapy. When enough beams are summed together, the PTV may be covered by a lower isodose such as 65 % that is often at the steepest part of the dose gradient. Choosing such a low prescription isodose line may have some theoretical disadvantages since a significant rind of normal tissue is in the PTV. Investigators at Fox Chase Cancer Center and at the University of Maryland use a 3-mm distance between the beam aperture and the PTV [64]. The prescription isodose line between 70 and 80 % is reasonable if the rind of normal tissue inside the PTV is small or can tolerate this high dose. Resultant high doses/hot spots occur in the center of the PTV, perhaps giving the highest dose to the center hypoxic

volume (although the potential benefit of this is unproven). Of note, the use of many beams for SBRT is not mandatory. For a peripheral liver tumor, three to five beams may be used to reduce the overall radiation path length through the liver. The use of segments within the beams can adjust the dose distribution to ensure that the hot spot is within the GTV while reducing the overall integral dose.

As the adverse effects of dosimetric errors are most pronounced with SBRT, appropriate methods to consider corrections for heterogeneities should also be used (see next section).

Typical prescription doses for SBRT range from 5 Gy in ten fractions to 20 Gy in three fractions. One to five fractions are most often used, with a dose per fraction usually greater than 6 Gy. The common feature to most of the SBRT fractionation schemes is that they are biologically potent. Multiple-fraction regimens have some radiobiologic advantages to single-fraction SBRT. Clinical data is not available to provide guidance for the most appropriate fractionation for each clinical scenario. However, when the PTV is in very close proximity to normal tissues that function serially, it is reasonable to consider prolonging fractionation to minimize the risk of toxicity to the serial function normal tissue.

It is a challenge to relate the prescribed dose to TCP, as inhomogeneous doses are generally used and various delivery and verification techniques are utilized. For a moving target not treated with image guidance, the actual delivered minimal dose to the tumor may be lower than the prescribed dose. Furthermore, there is heterogeneity in patterns of prescribing dose. One method to account for inhomogeneous dose distributions is to use equivalent uniform dose (EUD) to tumor for reporting [65]. Of course, accounting for individual patient motion in the dose distribution or eliminating motion would help ensure that the reported doses better reflect delivered doses as well. Unfortunately, it is not possible to account for motion in current commercially available planning systems.

Plan Evaluations

All conventional 3D plan evaluation methods apply to SBRT plan, but three criteria are specially considered: dose conformality, dose gradient, and dose heterogeneity.

Since SBRT delivers high dose (often >5 Gy per fraction) in a small number of fractions (≤5), high-dose conformality is required to minimize the dose to the normal tissue. A frequently used conformality index is defined as the ratio of volume receiving prescription dose to the PTV. A perfect plan should have conformality index equal to 1, i.e., PTV is covered by 100 % of prescription dose and no normal tissue receives the prescription dose or above. This is not realistic. Usually the conformality index of 1.3 is achievable. The index could be larger for smaller target or irregular target. In current or recently closed RTOG protocols of lung SBRT [10], for the target with maximum dimension between 2 and 7 cm, the conformality index was required to be less than 1.2, and the plan was considered as minor deviation with index between 1.2 and 1.4 but there is no good data to suggest complications are higher with a poor conformality index. As with similar data with intracranial SRS, target volume and proximity to critical structures usually trump the effect of conformality.

A sharp dose gradient out of PTV is desirable for SBRT plans. The dose gradient can be evaluated by how much %/mm or ratio of volume receiving 50 % of prescription dose to the PTV that was used in RTOG protocols of lung SBRT [10]. Usually a sharp dose-off isotropically is preferred although this can be limited to less degrees of freedom with non-coplanar fields, but the dose gradient can be larger in one direction if close to a critical structure.

The dose heterogeneity is probably not as important as the above two parameters, although it needs attention. To increase the plan conformality index and dose gradient usually increase the dose heterogeneity. The dose hot spot should be within the PTV, and the best place is the center of the PTV.

The dose constraints to critical organs are different with what are used in the conventional therapy. So far the dose tolerance is still immature and the dose to organ at risk should be evaluated carefully according to the peer-reviewed publications or protocols.

Treatment Planning System Considerations Related to Heterogeneity Corrections

The dose calculation heterogeneity correction is desirable for SBRT planning, especially for lung or spine SBRT. The treatment planning system (TPS) should be carefully evaluated to see if it is suitable for SBRT planning or specific site. Pencil beam algorithms have been discouraged for tumor sites surrounded by low-density tissue [59]. It has been reported that there was significant dose difference in the target periphery between pencil beam algorithm and superposition convolution algorithm for the lung SBRT [59]. Although the Monte Carlo simulation is the most accurate dose calculation algorithm, it may not be widely available for commercial TPS and take more time for dose calculation. The convolution superposition algorithm is more suitable considering the accuracy and calculation time is rather similar to Monte Carlo-generated plans.

Early in the North American experience with lung cancer, heterogeneity corrections were not used because tissue density correction dose algorithms were not widely available. In the absence of heterogeneity corrections, tumors completely surrounded by air experience a dose build-up effect due to the loss of electronic equilibrium, such that the periphery of a tumor is under-dosed, and a higher dose is required to achieve optimal cell kill [66]. Tumors that lack this air–tissue interface, such as tumors abutting the chest wall or central tumors, may have artificially high doses (“hot spot”) delivered

to the PTV, due to dose being delivered through low-density air using very long path lengths. Xiao et al. [67] applied heterogeneity corrections to the original treatment plans of 20 patients from RTOG 0236. They observed an increase in isocentric dose in all patients following the application of heterogeneity corrections. However, the mean volume of PTV receiving 60 Gy decreased from 95 to 85 %, and dose to 95 % of the tumor decreased by an average of 4.7 Gy [67]. Based on these findings, the use of heterogeneity corrections would be associated with larger hot spot doses but worsened overall tumor coverage, potentially leading to increased complications due to the high-dose areas and higher potential for failure due to underdosing parts of the tumor. This led the investigators to conclude that the RTOG standard dose should in fact be 18 Gy per fraction delivered to the 95 % isodose, for a total dose of 54 Gy. Notably, these patients all had peripherally located tumors.

Investigators at the University of Maryland repeated this work on patients with peripherally and centrally located lung tumors. This study shows that dose to the internal target volume (ITV) increases with the application of heterogeneity corrections and the effect was even greater with centrally located tumors and larger. In centrally located tumors, where more lung parenchyma is located between tumor and body surface, intervening tissue density is overestimated. When this is corrected, dose to the tumor increases, an effect observed in this study. This too is true of larger tumors, where increased beam widths traverse more parenchyma prior to reaching the PTV. Given the data above, the inclusion of central tumors in this sample may in part explain why the application of heterogeneity corrections led to an increase in D_{95} in this study, versus a drop in D_{95} as observed in the paper by Xiao et al. [67], in which central tumors were excluded.

Without heterogeneity corrections applied to treatment plans, a higher dose must be prescribed to achieve adequate dose to the tumor, which also results in a higher dose to the surrounding parenchyma. This increases the risk of adverse outcomes, which may help to explain the increased complications seen in the initial Indiana experience. Based on these results, the use of heterogeneity corrections allows the prescription of a lower total dose and dose per fraction, with a comparable dose to the tumor. This less aggressive dose prescription may allow safer yet equally efficacious treatment of NSCLCs.

Image Guidance

Overview

Image guidance at the time of treatment can improve setup accuracy, reduce PTV margins, and irradiate the volume of normal tissue, facilitating safe dose escalation.

Traditionally, surrogates for the target have been used in guiding the placement of treatment fields. For example, skin marks for patient position are routinely used for initial patient setup in practice. For some clinical situations, the use of skin marks to align the patient can be done with high precision. However, in most body tumors, the internal structures cannot be accurately localized with the use of skin marks. It has been reported the random setup error is up to 6.6 mm for pancreatic cancer patients receiving SBRT based only on body marker. The use of bony anatomy with electronic portal imaging is another standard practice in radiation therapy. However, for many clinical situations, the bony anatomy is not well correlated with the internal tumor position. Options for locating internal anatomy include the use of implanted radiopaque fiducial markers as surrogates for the target, tissues adjacent to the tumor, or the tumor itself. Fiducial markers may also be used to measure organ motion and/or track/gate the beam.

Many of the published reports of SBRT have been on patients treated with conventional linear accelerators. However, more specialized treatment units are now available with the potential to allow soft tissue image guidance and reduced PTV margins. Examples of such systems include a lightweight and robotic linear accelerator (CyberKnife; Accuray, Sunnyvale, CA) and modified linear accelerators to allow image guidance including accelerators such as Novalis (BrainLAB, Inc., Westchester, IL), Synergy (Elekta Oncology, Stockholm, Sweden), TrueBeam and Trilogy (Varian Medical Systems, Palo Alto, CA), Artiste (Siemens, Concord, CA), and TomoTherapy (Madison, WI).

Image-Guidance Strategies (Pretreatment)

Imaging at the time of treatment can be used for localization for guidance, verification, and also as a quality assurance (QA) tool that is evaluated by the treating physician prior to each treatment. Verification that the appropriate dose is actually delivered is also important for SBRT. Soft tissue imaging at the time of treatment can allow a measurement of the impact of geometric uncertainties (such as organ deformation) at the time of treatment. When image guidance and repositioning are used, imaging after repositioning should be used to ensure the positioning moves were made in the correct direction.

When repositioning moves are required due to changes in internal organ position, replanning is not routinely conducted. However, when substantial changes in organ position and or tumor size or breathing pattern occur, the dose delivered may be altered due to changes in radiation path lengths and position of organs with difference heterogeneities. The magnitude of dosimetric differences due to such changes should be studied to better define in which situations replanning may be of benefit. In addition, when soft alignments are utilized, the treating physician should also ensure the volume visualized on the volumetric imaging is similar to the ITV

generated on the 4D CT as differences may be related to different breathing patterns from day to day and may not improve alignments.

Two-Dimensional Image-Guidance Equipment

Orthogonal megavoltage (MV) portal films and more recently images from electronic portal imaging devices (EPIDs) have traditionally been used for image guidance and may be appropriate for targets adherent to the bones. MV images of large fields of view can be obtained with 2–8 monitor units (MUs) per image. These images not only can guide therapy but also can verify the shape and orientations of the treatment fields. If radiopaque fiducial markers are inserted in or near the tumor, the fiducial markers themselves may be used for guidance. Other alternatives for guidance include using surrogates that are in close proximity to the tumor, for example, the diaphragm as a surrogate for liver tumors [68, 69]. An example of an anterior–posterior (AP) MV image for liver cancer guidance, in which the diaphragm is used for cranial–caudal positioning.

Due to the low contrast of MV radiographs and the doses delivered with repeat MV imaging, orthogonal kV radiographs and kilovoltage (kV) fluoroscopy have also been used for image guidance of tumors and/or fiducial markers, either immediately prior to each radiation fraction [68, 69] or throughout radiation delivery [58]; kV X-ray tubes may be ceiling or wall mounted or attached to the linear accelerator.

With both MV and kV orthogonal imaging, alignment tools registering the images to digitally reconstructed radiographs (DRRs) can improve the accuracy and efficiency of image matching to determine the offsets in position. Such alignments tools include template matching tools based on therapists' visualization of anatomy and/or automated image registration of the region of interest (e.g., mutual information). Decision rules including tolerance levels for repositioning must be integrated with the overall system.

Three-Dimensional Volumetric Image Guidance

Technological advances allowing volumetric imaging allow image guidance immediately prior to treatment using the tumor or a soft tissue organ in close proximity to the tumor for guidance, rather than the bony anatomy. Advantages of volumetric imaging systems include that adjacent normal organs can also be visualized for more accurate avoidance of critical structures. Some of these volumetric imaging techniques can also measure tumor motion due to breathing.

Since the soft tissue can be visualized with three-dimensional volumetric images, it is possible to set up the patients based on the tumor target or organ at risk if which has more priority during the treatment. The pitfall of this strategy is that it may introduce the large setup uncertainty for target which has respiratory-induced motion. Currently, the CT scanner is fast enough to image the moving target on one breathing phase. The CBCT is slow and the moving target is more similar to internal moving target (ITV) on CBCT images. The in-room CT is actually a CT scanner and the moving target similar to one breathing phase. If the patient is aligned based on the target between planning CT and CBCT/in-room CT, the perfect target match may introduce the errors due to the difference in breathing phases between planning CT and CBCT/in-room CT. The correct strategy is to align the patient based on the bony structure and make sure that the target acquired through CBCT/in-room CT is within the PTV on the planning CT.

In-Room CT

The placement of a diagnostic CT scanner in the treatment room with a known geometric relationship to the linear accelerator is one approach for volumetric imaging immediately prior to treatment with the patient in their immobilization device. Uematsu et al. have used this approach to treat liver and lung cancers with SBRT. Uematsu et al. reported that with repeat CT for frameless head and neck cancer radiotherapy, there was a geometric vector error ranging from 0.1 to 0.9 mm [70]. Multiple manufacturers have developed products of this type, including Siemens' Primatrom, Mitsubishi's accelerator in combination with a General Electric CT scanner, and Varian's ExaCT targeting system [71–73]. All systems place the CT scanner in close proximity to the linear accelerator, allowing the couch to be moved from the imaging position to the treatment position. The CT scanner gantry is often translated during acquisition to minimize couch motion. Accuracy has been reported to be under 0.5 mm [72], and it has been reported to be improved with fiducial markers from 0.7 to 0.4 mm [71].

Advantages of in-room CT include that state of the art, diagnostic-quality CT can be used for optimal image quality and robustness. Disadvantages of this system are that the imaging and treatment isocenters are not coincident. Accuracy of motion from the CT scanner gantry, the accelerator couch, and the coincidence of the CT and linear accelerator isocenters needs to be verified. Limiting patient movement between imaging and treatment (e.g., couch retraction <1 mm) should improve setup accuracy; however, organ motion between imaging and delivery may occur.

kV Cone Beam CT

Jaffray et al. [74] first described the concept of cone beam CT (CBCT) for image-guided radiation therapy in 1997. CBCT refers to combined kV X-ray imaging and MV radiation delivery in one integrated gantry-mounted system. Advancements

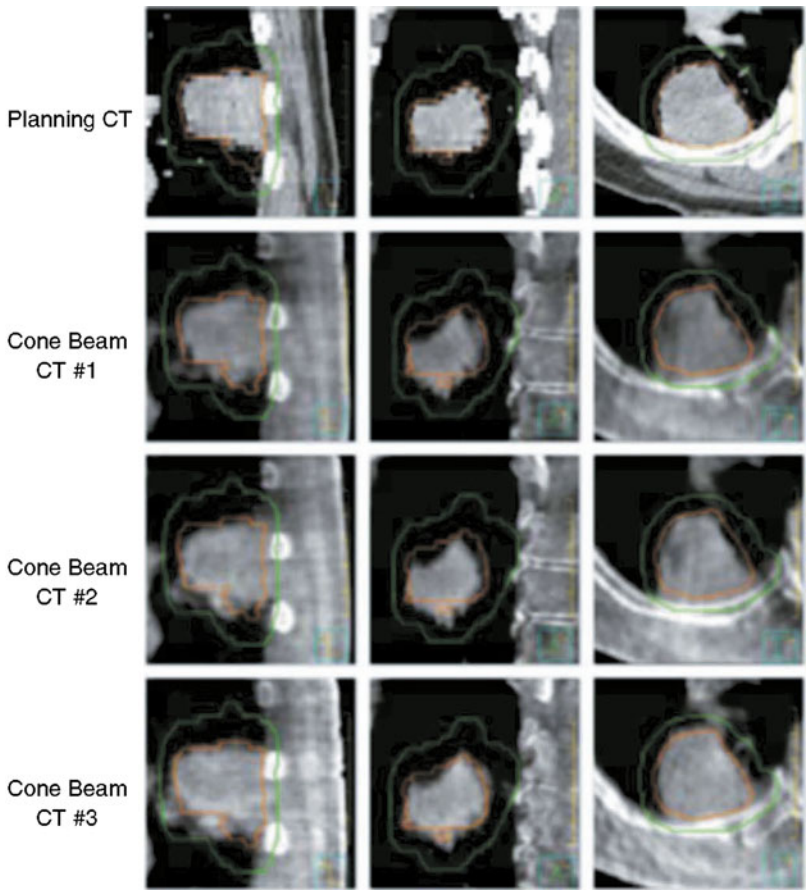

Fig. 13.2 Planning CT and kV cone beam CT from each lung cancer SBRT fraction. GTV from the planning CT scan is shown in *orange* and PTV in *green*

in large-area flat panel detector technology facilitated volumetric imaging to be acquired in a single rotation of the linear accelerator gantry. Planar kV images projections are obtained as the gantry rotates about the patient on the linear accelerator table, over 30 s to 4 min. CBCT three-dimensional volume reconstruction images may then be obtained for position verification or for image guidance (see Fig. 13.2). Geometric calibration methodologies for CBCT systems [75] and quality assurance recommendations [74] have recently been proposed.

Doses delivered to obtain CBCT scans typically range from 0.5 to 2 cGy. Two vendors have developed kV CBCT systems: Elekta Synergy and Varian Trilogy and TrueBeam. In addition to providing volumetric imaging for verification and guidance, these systems have the ability to be used for real-time kV tracking; the latter application has not been used clinically.

Similar to in-room CT, artifacts may occur with kV CBCT reconstructions due to high Z structures such as surgical clips, hip prostheses, and dental fillings. Methods to reduce these artifacts have been developed.

MV Cone Beam CT

CT imaging using MV beams has also been explored for more than 20 years [76, 77] and has also been made possible with advances in portal imaging technology. Advantages of MV cone beam CT are that the treatment MV beam is used to obtain the imaging, requiring less modification to the linear accelerator; the electron density estimates for treatment planning are accurate; and there is no high Z artifact that is associated with kV imaging.

MV cone beam CT has been used to aid in lung cancer SBRT, as described by Nakagawa et al. in 2000. MV CT-aided lung SBRT was used for treatment of 22 lung tumors [78].

Pouliot et al. recently reported the feasibility of acquiring low-exposure megavoltage CBCT. Phantom and pig cadaver head and neck images were acquired using a linear accelerator dose rate of 0.01–0.08 MU per image, for a set of 90–180 projections, acquired in 1–2° increments over 45–60 s. MV cone beam CT scans were obtained with doses of approximately 5 cGy. Despite the low efficiency of this system, visibility of high-contrast structures, such as air and bone, was reasonable [79].

MV TomoTherapy

MV TomoTherapy combines tomographic scanning capabilities, from a conventional CT detector, with a linear accelerator mounted on a rotating gantry. Simpson described the initial development of an MV CT scanner for radiation therapy in 1982 [76]. More recently, the TomoTherapy treatment platform has become available for image guidance and verification. The MV treatment beam is used to obtain imaging, with a lower energy, 3.5 MV instead of 6 MV. Computer-controlled multileaf collimators, also on the rotating gantry, have two sets of leaves that open and close to modulate the radiation beam while the couch advances the patient through the gantry bore, for helical intensity-modulated radiation therapy (IMRT).

Similar to MV cone beam CT, there are no high Z artifacts with MV TomoTherapy.

Image-Guidance Strategies (During Treatment)

Real-Time Tumor Tracking

Real-time tumor tracking while the radiation beam is on is another approach to reduce adverse effects of organ motion. An elegant highly integrated tracking system consisting of four ceiling-mounted fluoroscopic X-ray tubes and four floor-mounted flat panel imagers in the treatment room allowing visualization of radiopaque markers in tumors was first described by Shirato et al. [58]. This system has a temporal resolution of 30 frames per second and a precision of 1.5 mm. The linear accelerator is triggered to irradiate only when the fiducial marker is located within a predefined volume. This system has been used for image-guided radiation therapy of lung, liver, and paraspinal malignancies.

As an alternative to turning the radiation beam off when the tumor moves outside the treatment region, multileaf collimators, the couch position, or the entire accelerator on a robotic arm may move with the tumor to ensure adequate tumor coverage (e.g., CyberKnife image-guided radiosurgery system). The latter lightweight (330 lb) linear accelerator mounted on a robotic arm uses 6 MV, 5- to 60-mm collimators, and a dose rate of 300–400 MU per minute, combined with dual orthogonal fluoroscopy tubes to track radiopaque markers in or near the tumor at a preset frequency. When the beam is on, infrared external surrogates are continuously monitored, while the internal anatomy is monitored every few seconds with kV imaging. The external surrogates are used for determining the breathing model, and the model is updated based on the X-ray data obtained every few seconds. The robotic linear accelerator responds to motion by moving to an appropriate position, within a range of ±10 mm x, y, z and ±1° pitch and roll, ±3° yaw. This system was found to have a 0.3-mm accuracy when tested in phantom studies. Disadvantages of this system include the need for fiducial markers, long potential delivery times (up to 90 min), lack of suitability for large tumors with motion more than 10 mm, and highly inhomogeneous dose distributions.

Another system (Novalis: BrainLAB, Heimstetten, Germany) also acquires kV orthogonal images and matches the images to DRRs obtained from the planning CT. The imaging axes are not coincident with isocenter, and a translation of patient position is required between imaging and treatment. Accuracy of this system has been reported to be within 3 % and 3-mm distance to agreement.

Recently, wireless transponders and infrared cameras to track tumors have also been proposed as an imageless localization system (Calypso Medical Technologies, Seattle, WA).

SBRT Patient Safety

Since SBRT gives very high dose and uses much smaller planning margin than conventional therapy, more caution must be given to avoid catastrophic dose delivery. The patient safety has got more and more attention in radiation therapy society. Recently, the ASTRO SRS/SBRT white paper was published to address SRS/SBRT quality and safety considerations. This chapter presented the personnel requirement and training for radiation oncologist, medical physicist, medical dosimetrist, radiation therapist, and administrator; presented the technology requirements of simulation, planning, and localization; and addressed the SRS/SBRT system acceptance and commissioning.

The report of AAPM TG101 also has recommendations for SBRT patient safety issue. It recommends that at least one qualified medical physicist presents during first fraction of SBRT treatment and the qualified medical physicist should be available for the following fractions. It also recommends that the radiation oncologist should approve the image guidance before each fraction treatment. The therapist should be well trained for the SBRT procedure.

Equipment Quality Assurance

The equipment of SBRT mainly include the linac system and imaging system. The QA frequency is daily, monthly, and annually. Usually the radiation therapist performs the daily QA and the qualified physicist reviews and approves it, and the qualified physicist performs the monthly and annual QA. Apparently SBRT linac has tighter tolerance than the linac only for conventional therapy. The report of AAPM Task Group 142 [80] published recommendations for SRS/SBRT linac QA. The main recommendations about accuracy tolerance are summarized here. It recommends that the laser, the couch movement indictor, collimator size indicator, collimator rotation isocenter, couch rotation isocenter, gantry rotation isocenter, and coincidence of radiation and mechanical isocenter have to be within 1 mm. The couch rotation

indictor has to be within 0.5°. The imaging system includes kV/MV imaging and kV/MV cone beam CT. It recommends that the imaging and treatment coordinate coincidence should be within 1 mm. For cone beam CT, the geometric distortion should be within 1 mm, and the contrast, spatial resolution, HU constancy, uniformity, and noise should agree with the baseline.

Clinical Outcomes

The next several sections will review the most common clinical sites where SBRT/SABR is delivered most commonly where pertinent issues related to patient selection, simulation, treatment planning, and morbidity specific to that clinical site. This data should be used with caution when extrapolating to other locations (i.e., primary liver versus metastatic liver since the background normal tissue is already partially injured) but will be good starting point prior to treating a unique site.

Stereotactic Ablative Radiotherapy for Lung Tumors

Lung cancer is the second most common cancer diagnosis and the most common cause of cancer death for both genders. In 2012, there was an estimated 226,160 new lung cancer diagnoses in the United States and 160,340 deaths [81]. Of the 15 % of patients diagnosed with early-stage lymph node-negative NSCLC, the 5-year relative survival is only 52 %. The current standard of care for these patients is surgery [82]. When a patient cannot tolerate or refuses surgery, radiation therapy is an excellent alternative with current literature suggesting outcomes following SBRT/SABR similar to surgery. For patients with severe comorbidities, it is important to understand what the natural history of early-stage disease is. Approximately 50 % of patients require treatment for symptoms at 1 year and on average 50 % die of lung cancer at 2 years without treatment [83].

Patient Selection

This approach is widely accepted as the current standard of care for peripheral T1 or T2 tumors or certain T3 tumors (i.e., invading the chest wall) which measure less than 5–7 cm without any nodal involvement. Central lesions may have a higher complication rate in comparison to peripheral tumors based on the initial phase II experience published out of Indiana [8]. In their single institution experience, "excessive toxicity" was reported for patients with tumors located within 2 cm of the proximal respiratory tree where the rate of grade 3 and above toxicity was significantly higher among patients with central tumors. This increase in toxicity may be related to dose and dose per fraction. Stephans et al. [84] reported the experience at Cleveland Clinic, which clearly illustrates the effects of the higher biologic effective dose (BED) on morbidity. Their institutional practice of SBRT initially used 10 Gy × 5 fractions and subsequently changed to the RTOG standard (18–20 Gy × 3) when RTOG 0236's results were initially reported. The local control rates showed no difference between the two schemas, although they did experience a high rate of chest wall morbidity with the higher BED regimen (18 % versus 4 %, $p = 0.028$). In addition, follow-up from the initial Indiana experience treating central tumors reported lower grade 3 and higher side effects when >3 fractions were used as opposed to three fraction (26.3 % versus 7.7 %) [85]. However, caution is still indicated. Washington University [86] has completed a phase I study demonstrating 60 Gy in five fractions is safe for treating central tumors and is currently accruing to a phase II study. Many retrospective series also suggest a five fraction is safe in treating centrally located tumors [87]. In addition, a multi-institutional phase I/II [88] RTOG study is currently nearing completion using a similar fractionation schedule as the Washington University. Led by Videtic et al. [88] from the Cleveland Clinic, the RTOG has currently completed testing two less aggressive schemas (12 Gy × 4 fractions and 34 Gy × 1 fraction) in a randomized phase II trial, specifically looking at morbidity at 1 year as the primary end point as local control is expected to be 90 % in both arms (RTOG 0813). The less aggressive regimen will then be compared to the current RTOG standard which is a subsequent phase III trial. There is no lower limit of lung function based on pulmonary function tests that predicts poor outcomes [89]. One clinical entity that may have a higher risk of pulmonary injury is patients with interstitial pulmonary fibrosis. Onishi et al. [90] described 24 patients who died of fatal pneumonitis in the large multi-institutional experience. Seventeen of the 24 patient had IPF with 1 of the patients with usual interstitial pneumonia. The absolute risk of fatal pneumonitis for this cohort of patients in Japan is not known, but from Washington University described a 20 % risk of pneumonitis in patients with IPF. So a diagnosis of IPF is not a contraindication for SBRT but does appear to be at a higher risk of pneumonitis.

Treatment Planning

During the CT simulation, 3-mm slice thickness or less is preferred. IV contrast may be helpful for tumors close to the brachial plexus or for central tumors adjacent to vasculature. The gross tumor volume (GTV) is contoured on pulmonary windows, although soft tissue windows are helpful for tumors adjacent to the chest wall and central lesions. Contouring all the spiculations on lung windows is controversial and not uniformly performed. At the University of Maryland, only the bulky component of the spiculation is

contoured (2-mm thickness) based on unpublished literature suggesting that it is uncommon that these radiographic findings correlate with clinically significant disease and is covered with subclinical doses in the area of dose falloff [61]. There are institutional preferences regarding the use of a margin for microscopic extension and creation of a CTV. In RTOG 0236, it was specified that the GTV was equivalent to the CTV. Assessment of respiratory motion and creation of an ITV is preferred to limit the PTV margins similar to SRS in the brain. The ITV can be assessed with a 4D CT scan or with fluoroscopy to track the tumor or a fiducial implanted into the tumor. A margin of 0.5 cm to create the PTV from the ITV is common. If an ITV is not created, population-based margins of 0.5 cm axially and 1.0 cm in the craniocaudal directions were used historically in the Indiana experience and RTOG 0236. However, the use of patient-specific tumor motion is preferred. This can be performed by fusing maximum inspiration and expiration breath-hold scans to a free breathing CT, obtain a "slow" CT simulation, if 4D CT is not available. 4D CT has been demonstrated to result in smaller PTV volumes than any of the other described options [91]. If there is significant respiratory motion, some have advocated for managing this with abdominal compression or breath-hold maneuvers. The benefit of abdominal compression is likely to be greatest for lower lobe tumors. However, abdominal compression may increase tumor motion in some cases and should be considered on an individual basis and there are several studies which demonstrate increased failure with the use of abdominal compression and gating [92]. At the University of Maryland, a CTV margin of 3 mm is added based on the unpublished work from Fox Chase Cancer Center which evaluated 25 consecutive patients who underwent a lobectomy or sublobar resection for a curative procedure for tumors <3 cm in maximum dimension and also had a diagnostic CT scan for review. Based on a comparison of CT and microscopic pathology review, the entire microscopic extent of disease was covered when 3 mm was added to the maximum extent of the disease contoured on standard lung windows without chasing the spiculations in 95 % of the cases. An additional 3 mm was added for setup error based on obtaining a daily CBCT prior to each treatment.

Interfraction setup variation is reduced with image-guided radiotherapy (IGRT). This can be performed by matching fiducial location, which is vital to technologies which do not use volumetric IGRT, and/or creating a CBCT with the patient immobilized. These pretreatment images are compared to the simulation images and adjusted as appropriate. Fusion of the CBCT with the simulation CT using bony anatomy is recommended, as there is minimal change in the target centroid position relative to the skeletal frame [93]. The differences in patient position based on matching with bony anatomy versus soft tissue can be off by upwards of 8 mm on average but this is primary based on our medically inoperable patients who are likely to have emphysema and poorly functioning diaphragms [94]. Alignment using soft tissue can be performed if imaging acquired on cone beam imaging is similar to that generated by the 4D CT-based ITV. If the volumes do not match, then the treating physician needs to consider that the patient's breathing pattern may be different from the day of the initial 4D CT. This difference may not be reflected accurately on the CBCT and alignment based on soft tissue may therefore be inaccurate potentially leading to a geographic miss. In this situation, a bony alignment is preferable and treatment can be delivered if the volume is safely within the PTV on the CBCT. If it is outside the volume, a repeat 4D CT is preferred.

At the University of Maryland, consideration of the accuracy of cone beam imaging is considered to be 2 mm such that a shift will be performed only if the shift is 3 mm or more based on the work from Princess Margaret Hospital [95].

Fractionation

There are two predominant fractionation schedules used in the United States: the Japanese approach (12 Gy×4) [96] and the original Indiana approach developed by Dr. Timmerman (18–20 Gy×3) [6, 8]. Outcomes and dose–response will be discussed under clinical outcomes. In the original Indiana series that led to RTOG 0236, dose is calculated without heterogeneity corrections. When these are applied, the dose is on average 10 % lower for the subset of patients treated on the study [22]. The prescription isodose line covering the PTV is usually 60–90 % depending on the block edge margin (2–3 mm, respectively) used on each beam's eye view. Typically a minimum of 7–9 non-coplanar, non-opposing beams are required to obtain adequate dose falloff to minimize risk of morbidity (see Fig. 13.3). Plans are assessed by dose conformality similar to strategies utilized in the brain where the primary goal is to devise the most conformal plan to the PTV with the secondary goal to minimize the volume receiving 50 % of the prescription dose. The currently accruing RTOG protocols recommend that 95 % of the PTV be covered by the prescription isodose and 99 % of the PTV receives a minimum of 90 % of the prescription dose. A prescription isodose to PTV volume (PITV) ratio of 1.2 or less is recommended, except for tumors smaller than 1.5 cm as this constraint is difficult to meet. Additional RTOG recommendations are in place to limit toxicity to normal structures. This includes no more than 15 % of the PTV volume of tissues outside the PTV receiving more than 105 % of the prescription dose. The so-called intermediate dose spillage is limited by imposing criteria on the ratios of the 50 % prescription isodose volume to the PTV volume and the maximal dose at 2 cm from the PTV, which are dependent on PTV volume. This uniform dose falloff may be important especially in the parenchyma of the lung where subclinical disease may be present.

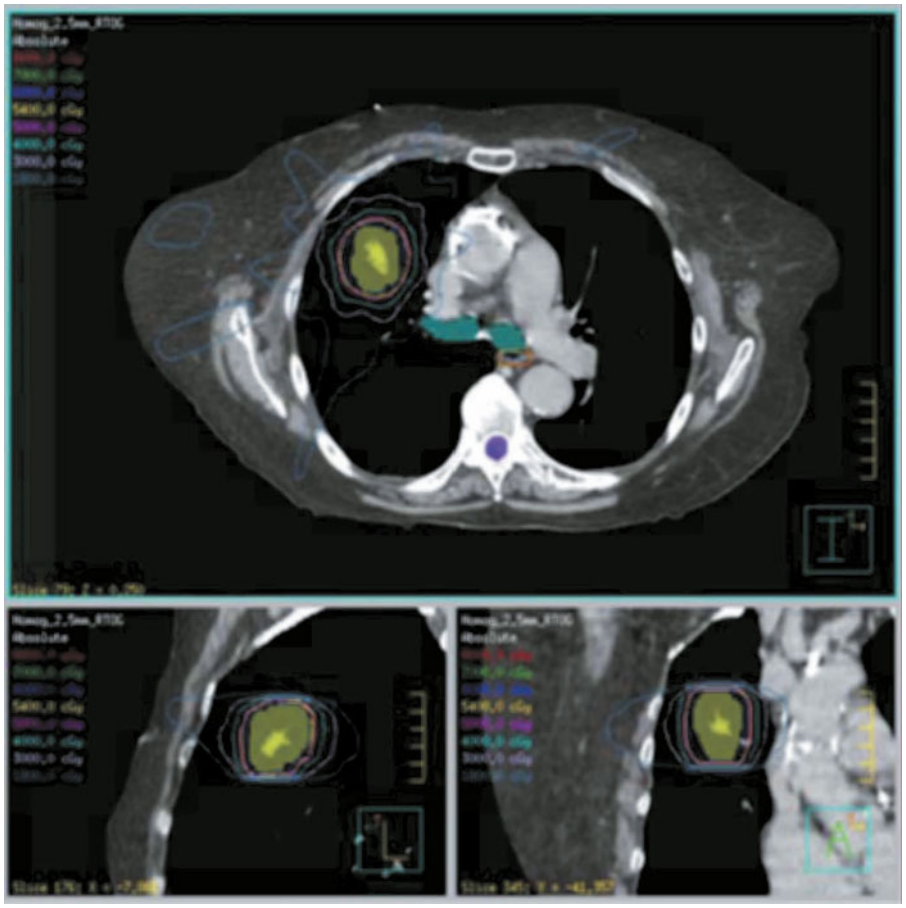

Fig. 13.3 SBRT dose distribution for lung cancer

Clinical Outcomes

SBRT/SABR has been most widely studied in primary and metastatic lung cancer. A summary of clinical data is shown in Tables 13.1 and 13.2 and some of the major studies are discussed in greater detail below.

Initial reports from the Karolinska Institute and Japan, who first reported the use of extracranial stereotactic radiotherapy included patients with lung cancer and lung metastases. In 2004, Onishi et al. reported a large multi-institutional experience from 13 institutions in Japan of nearly 250 patients that had a major impact on clinicians taking care of lung cancer patients. Using a variety of techniques and fractionation scheme, local control was found to be 86 % at 5 years when adequate dose was delivered as compared to 50 %. In addition, the side effect profile was remarkably low. Onishi suggested that the dose–response was based on delivering a BED greater than 100 Gy [25, 97]. This fraction may be inadequate for tumors >3 cm and for lung metastases where investigators advocate 12 Gy×5 or 18–20 Gy×3 [98, 99]. A BED of greater than 100 was an important factor for local control even for centrally treated lung tumors [100]. In a large pooled analysis from the Elekta consortium of over 500 patients, a BED of 105 or greater predicted was confirmed to predict for an excellent local control with no clear benefit from further dose escalation [99]. Regional nodal failures and distant metastases are more common for central tumors and tumors >3 cm.

The North American experience was pioneered by Dr. Timmerman at Indiana University where a series of prospective protocols were conducted which led to the development of all of the RTOG SBRT trials. His initial phase I dose escalation study included 37 medically inoperable patients with Stage I NSCLCs (<7 cm). The dose was escalated from 24 Gy in three fractions in 2 Gy/fraction intervals to 60 Gy and higher in three fractions. The maximum tolerated dose was not reached and 87 % of patients had tumor response, including 27 % with a complete response [6] and a dose–response curve where a local control of >90 % was achieved when 18 Gy or higher fraction was used. A phase II study was conducted using 60 Gy in three fractions for T1 tumors and 66 Gy in three fractions for T2. Local control at 2 years was 95 % and overall survival was 54.7 % at 2 years. Toxicity was significantly greater for those treated with central tumors [8] and was subsequently excluded from RTOG 0236.

Table 13.1 Selected results of primary non-small cell lung cancer treated with SABR

Reference (year published)	No. patients	Patient population (all N0 M0)	Total dose (no. fractions)	Median follow-up (months)	Local control	Regional control rate (%)	Distant metastasis rate (%)	Overall survival
Uematsu (2001) [23]	50	18 pts received 40–60 Gy prior to SABR	50–60 Gy (5–6)	36	94 %	96	14	66 % at 3 years
Wulf (2004) [30]	20	10 % T1 50 % T2 40 % T3	30–37.5 Gy (3)	11	95 %	NR	25	32 % at 3 years
Nagata (2005) [19]	45	71 % T1 29 % T2	48 Gy (4)	30	98 %	93	20	At 3 years: 83 % for T1 and 72 % for T2
Timmerman (2006) [20]	70	50 % T1 50 % T2	60 Gy (3)	17.5	95 % at 2 years	100	10	55 % at 2 years
Yoon (2006) [34]	21	62 % T1 38 % T2	30–48 Gy (3–4)	13	86 %	100	5	51 % at 2 years
Onishi (2007) [24] [25]	257	Multi-institutional review 63 % T1 37 % T2	18–75 Gy (1–22)	38	86 %	89	20	47 % at 5 years
Hof (2007) [32]	42	40 % T1 50 % T2 10 % T2	19–30 Gy (1)	15	95 % at 1 year; 68 % at 2 years	95	31	65 % at 2 years
Fakiris (2009) [35]	70	49 % T1 51 % T2	60–66 Gy (3)	50	88 % at 3 years	91	13	43 % at 3 years
Baumann (2009) [36]	57	70 % T1 30 % T2	45 Gy (3)	35	93 %	95	16	60 %
Timmerman (2010) [29]	55	80 % T1 20 % T2	60 Gy (3)	34	91 %	87	22	48 % at 3 years
Ricardi (2010) [37]	62	69 % T1 31 % T2	45 Gy (3)	28	88 % at 3 years	94	24	57 % at 3 years
Bral (2011) [28]	40	65 % T1 35 % T2	Central: 45 Gy (3) Peripheral: 60 Gy (3)	16	92 %	95	15	52 % at 2 years

Staging is AJCC sixth edition
NR not reported

Timmerman et al. reported the multi-institutional phase II experience including 55 medically inoperable, NSCLC patients with T1 (80 %) and T2 (20 %) N0 M0 tumors less than 5 cm treated to 60 Gy in three fractions. After a median follow-up of 34 months, the tumor control rate was 97.6 %. At 3 years, the involved lobe (local) control rate was 90.6 %, the local regional control rate was 87.2 %, and the distant metastasis rate was 22.1 %. Median survival was 4 years [10]. This work has now led to subsequent studies at the RTOG (0618 and 1014) which are now challenging surgery as the standard of care for early-stage lung cancer.

Complications

Despite the majority of the patients on these studies being medically inoperable with significant comorbidities, there are relatively few grade 3–5 toxicities related to radiotherapy. Normal tissue constraints used in RTOG 0618 and 0915 are shown in Table 13.3, although these values are more conservative than the constraints employed by the Japanese. Dose–volume analyses confirming and disputing these values are described below.

Pneumonitis is the dose-limiting complication after conventional radiation therapy for lung cancer. It is a clinical diagnosis of exclusion, consisting of cough, fever, pleuritic pain, and dyspnea, with occasional respiratory failure and general inflammation and can be extremely difficult to differentiate between a COPD exacerbation, an atypical pneumonia, and a viral infection. Characteristic radiographic findings are often present, typically in the distribution of the radiation fields. A prolonged course of prednisone is the typical treatment using 50–60 mg/day initially followed by a slow taper. Based on the low incidence, arbitrary constraints

Table 13.2 Selected results of lung metastases treated with SABR

Reference (year published)	No. patients (no. lesions)	Patient population	Total dose (no. fractions)	Median follow-up (months)	Local control	Overall survival
Wulf (2004) [30]	41 (51)	Primary site: 45 % lung 10 % breast 8 % colorectal 8 % kidney 8 % sarcoma	30–37.5 Gy (3) or 26 Gy (1)	9	90 %	33 % at 2 years
Yoon (2006) [34]	53 (63)	Primary site: 26 % lung 23 % liver 19 % colorectal 8 % esophageal	30–48 Gy (3–4)	14	82 %	NR
Hof (2007) [38]	61 (71)	Primary site: 51 % lung 30 % other histologies 12 % colorectal	12–30 Gy (1)	14	89 % at 1 year	65 % at 2 years
Milano (2008) [39]	121 (293)	Primary site: 32 % breast 26 % colorectal	Most 50 Gy (5)	41	67 % at 2 years	50 % at 2 years
Norihisa (2008) [40]	34 (43)	Primary site: 44 % lung 26 % colorectal	48–60 Gy (4)	27	91 % (crude)	84 % at 2 years
Rusthoven (2009) [41]	38 (50)	1–3 lung mets, < 7 cm	48–60 Gy (3)	15	96 % at 2 years	Median 19 months
Ricardi (2012) [42]	61; 74 % single nodule	Primary site: 46 % lung 21 % colorectal	36–45 Gy (3–4) 1 pt 26 Gy (1)	20	89 % at 2 years	67 % at 2 years

NR not reported

Table 13.3 SABR lung normal tissue maximal point dose constraints for three and four fraction regimens based on RTOG 0618 and 0915, respectively

	Three fractions (20 Gy × 3)	Four fractions (12 × 4 Gy)
Spinal cord	18 Gy (6 Gy per fraction)	26 Gy (6.5 Gy per fraction)
Esophagus	27 Gy (9 Gy per fraction)	30 Gy (7.5 Gy per fraction)
Brachial plexus	24 Gy (8 Gy per fraction)	27.2 Gy (6.8 Gy per fraction)
Heart/pericardium	30 Gy (10 Gy per fraction)	34 Gy (8.5 Gy per fraction)
Trachea/ipsilateral bronchus	30 Gy (10 Gy per fraction)	34.8 Gy (8.7 Gy per fraction)
Skin	24 Gy (8 Gy per fraction)	36 Gy (9 Gy per fraction)

were developed. The RTOG used the percent of lung receiving 20-Gy total or more (V20) be less than 10 % in RTOG 0236 and 0618. RTOG 0915 which uses a less aggressive regimen used absolute volumes as opposed to percentages of the total where more than 1.5 L of the lung volume should receive 11.6 Gy in four fractions and the maximum 1.0 L should receive 12.4 Gy. Barriger et al. [101] reported the dose–volume analysis from the Indiana experience which included 273 patients treated with SBRT. The overall grade 2 and higher pneumonitis rate was seen in 9.4 % of their patients with the majority (7 %) graded as 2. The most important predictor of grade 2 and higher pneumonitis was the mean lung dose ($p = 0.02$) and V20 ($p = 0.03$). When comparing the RTOG cut point in V20 of 10 %, the investigators found that 10 % did not predict an increase in side effects ($p = 0.42$), but when the median value of 4 % was used, this increased the risk fourfold from 4 to 16 % ($p = 0.03$). Although their most recent update suggests a V20 cut point of 6.5 % continues to have a very low risk of pneumonitis. The majority of these patients were treated with a three-fraction approach. When using less aggressive schemas, no grade 3 or higher pulmonary events were reported by Nagata et al. in treating patients with 48 Gy in four fractions [96]. Onishi et al. reported a 5.4 % incidence of grade 2 and higher pneumonitis with no grade 5 events [97, 102]. Other, potentially permanent pulmonary toxicities after SABR include bronchial damage that can be associated with total obliteration of the airway lumen and downstream atelectasis. Tracheal

stricture and/or necrosis with subsequent lung collapse or injury is another toxicity that is possible after highly potent SABR to medial lung cancers is rare.

Chest wall pain and rib fracture have been reported in 7–15 % of SBRT/SABR patients. Taremi et al. created a nomogram using age, female gender, and dose to 0.5 cc of the ribs to estimate the risk of bone injury following SABR. In this study, 0.5-cc ribs receiving 60 Gy was associated with a 50 % risk of fracture [95]. Dunlap et al. found that the median interval to onset of severe chest wall pain and/or fracture following lung SABR was 7 months and the best correlate was the volume receiving 30 Gy. The authors recommended limiting the chest wall volume receiving 30 Gy in 3–5 fractions to less than 30 cc, but they similarly saw a high risk for the volume receiving >60 Gy suggesting fractionation may play a critical role [103]. Stephans et al. [104] reported the dose–volume analysis from Cleveland Clinic for their patients who received 60 Gy in three fractions without the use of heterogeneity corrections that the most important predictors of chest wall pain in the volume of chest all receiving 30 and 60 Gy should be kept below 25 and 3 cc, respectively. Welsh et al. [105] reported the MD Anderson experience using a less aggressive schema (50 Gy in four fractions) suggesting the volume receiving 30 Gy is also the most important predictor of grade 2 and higher pain, but the absolute volume cut point is higher (50–100 cc).

Brachial plexus and phrenic nerve injuries are extremely rare. Indiana University experience described seven brachial plexus injuries, of which four were grade 2, one grade 3, and one grade 4. When the dose was greater than the median dose (26 Gy over three fractions), the 2-year incidence of brachial plexus injury was 46 % versus 8 % ($p=0.038$) for lower doses [85].

Stereotactic Radiotherapy for Metastatic Tumors of the Spine

For information on stereotactic radiotherapy for metastatic spinal tumors, please see Chap. 45.

SBRT/SABR for Liver Tumors

SABR can be used to treat tumors originating from the liver, such as HCC and cholangiocarcinoma, as well as those that have metastasized from a different organ. Liver tumors from metastatic disease occur more frequently than primary liver cancer, of which CRC is the most common [106]. In 2012, there was an estimated 28,720 new cases of liver and intrahepatic biliary duct cancer in the United States with an estimated 20,550 deaths. Although the 5-year relative survival rate for patients with cancer of the liver and bile ducts has tripled in the last several decades from 3 % in 1975–1977 to 15 % in 2001–2007 ($p<0.05$), most patients will die of their disease [81]. With approximately 748,300 new cases and 695,900 cancer deaths globally in 2008, primary liver tumors were the second most frequent cause of cancer death in men and the sixth in women [81]. The standard of care for HCC is surgical resection. For patients with cirrhosis, resection alone is problematic since the precipitating etiology is still present and subsequently orthotopic liver transplant (OLT) appears to have a superior outcome for select patients with reported 10-year survival rates of >70 % as it resects the tumor and corrects the underlying etiology [107, 108]. Unfortunately, only 30–40 % of HCC patients may be candidates for OLT or surgical resection [109]. If untreated, median survival from HCC is 6–12 months [110]. Similarly, select patients with metastatic disease to the liver from CRC appear to have better outcomes with complete surgical resection of all liver disease. These patients have a 5-year survival of 30–40 % [111]. Unfortunately, only 10–20 % of patients are resection candidates [112]. For individuals with unresected CRC, liver metastases have median survivals of 10–17 months which can improve to 20 months with systemic therapy [113–115]. For unresectable primary liver cancers, the use of radiofrequency ablation (RFA), radioembolization with yttrium-90 microspheres, cryotherapy, percutaneous ethanol or acetic acid injection, laser-induced thermal therapy, and high-intensity focused ultrasound have been studied [110, 116, 117]. SABR offers a completely noninvasive approach to treat primary and metastatic liver tumors not amenable to resection.

Treatment Planning

Planning SABR for liver tumors is more difficult for several reasons. IV contrast is vital for accurate tumor delineation and timing of administration is vital. In addition, as these tumors near the diaphragm and in nonsmokers commonly motion tumor motion can be significant. Therefore, trying to deliver contrast during a 4D CT can be extremely difficult to get an accurate tumor delineation and an accurate estimate of motion. As the liver has a dual blood supply, tumors can be fed either from the portal system or from the hepatic artery and depending on the tumor type tumor delineation can vary. HCC is typically hypervascular and fed from the arterial system and subsequently the arterial phase imaging with CT or MRI is necessary for proper delineation as opposed to liver metastases which are best visualized during the venous phase. MRI or FDG-PET scans can be fused to the CT to improve visualization of the tumor, which radiation oncologists define as gross tumor volume (GTV) although accuracy of the fusion is generally 1–2 mm. CT slice thicknesses of 2–4 mm are recommended to balance lesion detection rate and image noise [81]. On MRI, CRC liver metastases tend to be hypovascular and HCC demonstrates tumor arterial enhancement

with "washout" and a delayed enhancing pseudocapsule, restricted diffusion, and T2 hyperintensity [118]. A CTV is created by adding margin to the GTV for microscopic tumor extension. In a clinicopathologic correlative study in HCC patients, CT and MRI correlated equally with resected tumor specimens. The authors concluded that margins of 5 and 10 mm would have encompassed 93 % and 100 %, respectively, of the cases [119]. For CRC metastases, microscopic extension can be found 0.2–10 mm from the main tumor, with 80 % within 3 mm and 90 % within 6 mm [120].

Liver motion is predominant in the superior–inferior (SI) direction and can vary greatly among individuals and breathing patterns. SI liver motion ranges from 0.5 to 3.7 cm [121–123]. Average anterior–posterior (AP) and left–right (LR) liver tumor motion has been reported to be 1.0 cm (range: 0.4–2.2 cm) and 0.8 cm (range: 0.4–1.5 cm), respectively [124]. Liver tumor motion can be measured in several different ways by using (1) cine MRI, (2) fluoroscopy, or preferably (3) 4D CT scan. Fiducial placement is beneficial for several reasons when treating below the diaphragm with the only drawback being the rare, but real risk of tumor seeding along the insertion track. Fiducials, if placed in or near the tumor, can act as a surrogate for tumor location during the 4D CT scan or can be checked by fluoroscopy. In addition, fiducials can significantly improve image guidance. Even with volumetric IGRT, the lack of contrast difference in the liver makes it nearly impossible to visualize the tumor unless it is at the edge of the liver or near the gall bladder. Finally, fiducial placement is the only way tumor tracking could be performed adequately. By measuring organ motion, an appropriate margin can be added to the CTV to create an ITV. To reduce the size of the ITV margins, abdominal compression has been utilized by some to reduce diaphragmatic and liver motion. In a study by Heinzerling et al., abdominal compression almost halved tumor motion from 13.6 to 7.2 mm [125]. Notably, abdominal compression can increase AP motion due to liver deformation [126, 127]. An alternative to abdominal compression, which may not be tolerated by all patients, is tumor tracking or gating.

A PTV is created from the ITV to account for setup errors between radiation treatments. Interfraction reproducibility is improved by doing image-guided radiotherapy (IGRT) prior to each treatment. This is performed by matching fiducial location with kV imaging and/or creating a CBCT with the patient immobilized. These pretreatment images are compared to the simulation images and adjusted as appropriate, reducing interfraction motion.

Clinical Outcomes and Patient Selection

Local control rates of SABR for liver tumors range from 65 to 100 % at 1 year. Table 13.4 summarizes recently published articles for SABR of primary and metastatic liver tumors. The small number of patients in these trials and variations in eligibility criteria makes direct comparisons difficult. Inclusion criteria ranged from only primary or metastatic liver tumors to a combination of both. Two of these studies incorporated patients treated with SABR to liver lesions and other anatomic locations within the same report [128, 129]. Radiation dose may be based on estimates of toxicity risk [24, 130]. Additionally, some of the HCC patients underwent liver transplant after SABR [131, 132]. Child–Pugh (CP) class B patients were sometimes permitted, while other studies restricted to only class A patients. None included patients with CP class C. The fractionation schemes vary from a single large fraction up to ten fractions.

The ideal patient for liver SBRT has no extrahepatic disease with >700 cc of normal uninvolved liver, has adequate liver function (CP B or better) and is located >1.5 cm from a luminal gastrointestinal structure. The maximum tumor size is less than 6 cm for a metastasis or less than 8 cm for a primary HCC. Vascular involvement is not a contraindication. Absolute contraindications are patients with extrahepatic disease, >8 % of the liver involved with cancer, have a small liver (<500 cc), CP C, <0.5 cm from a luminal gastrointestinal structure or a tumor that is greater than 15 cm for a metastasis or greater than 20 cm for a primary HCC [133, 134].

Wulf [135], Rule [136], and Chang [137] demonstrated improvements in local control with dose escalation. A recent pooled analysis by Chang et al. of 65 patients with 102 metastatic CRC lesions treated to a median dose of 41.7 Gy in six fractions demonstrated local control of 65 % at 1 year and 55 % at 2 years. They estimated that doses of 46–52 Gy in three fractions were needed to have 1-year local control of more than 90 % [137]. In comparison to lung SBRT, patients with metastatic disease to the liver appear to have the highest control rates with the most aggressive regimens. Rusthoven et al. [109] have demonstrated the best local control using 60 delivered in three fractions where the local control was 92 % at 2 years including 100 % for tumors less than 3 cm. Wulf et al. demonstrated an improved response in patients treated with "high dose" which was defined as 26 Gy in one fraction or 36 Gy in three fractions ($n=26$) versus "low dose" which was defined as 30 Gy in three fractions or 27 Gy in four fractions ($n=25$) [135]. In a similar fashion Goodman et al. reported the single-fraction phase I from Stanford where better local control was seen with doses of 26 and 30 Gy as opposed to 18 and 22 Gy [138]. Rule et al. demonstrated greater than 90 % local control when 50 or 60 Gy was delivered in five fractions as opposed to lower doses based on their phase I experience [136]. As for the patients with HCC, 90 % local control has been more challenging due to the underlying liver disease having a major impact on tolerance of dose escalation. Lower doses have been associated with higher response rates compared to metastases; finding the appropriate dose for tumor control that will not precipitate liver toxicity is a challenge for HCC, especially when underlying liver function is poor (e.g., Child–Pugh B or C).

Table 13.4 Studies of SABR for liver lesions

Study (year published)	No. pts (lesions)	Pt population	Tumor size (range)	Dose (no. fractions)	Median follow-up (range)	Local control	OS	Toxicity
Herfarth (2001) [33]	37 (60) Inc: 56 mets, 4 primary liver tumors	Surgical intervention not possible	1–3 lesions. Max each lesion 6 cm Median 10 cc (1–132 cc)	14–26 Gy (1)	5.7 months (1–26.1)	71 % at 1 year (actuarial)	72 % at 1 year (actuarial)	No statistically significant changes in liver enzymes
Schefter (2005) [34]	18 mets, including 6 CRC mets	1–3 lesions, < 6 cm >700 mL normal liver receive < 15 Gy	Median aggregate GTV 18 cc (3–98)	36–60 Gy (3)	NR	NR	NR	No grade 3–5 toxicities
Choi (2006) [35]	20 HCC (20)	Single lesion CP Class A-B No extrahepatic disease	Mean 3.8 cm (2–6.5 cm)	50 Gy (5–10)	23 months (3–55)	80 %	70 % at 1 year 43 % at 2 years	No grade 3–5 toxicities
Mendez Romero (2006) [36]	25 (45) total	HCC or metastatic tumors, not eligible for other local treatment (RFA or surgery)	Median 3.2 cm (0.5–7.2 cm)	30.0–37.5 Gy (3) if mets, HCC without cirrhosis, or HCC <4 cm with cirrhosis	12.9 months (0.5–31)	94 % at 1 year	75 %	One grade 5 liver–HCC, Child B
	15 (31) CRC mets			25 Gy/5 or 30 Gy/3 if HCC >4 cm and cirrhosis		82 % at 2 years		Two grade 3 liver—met pts
	8 (11) HCC	CP Class A-B				For HCC, 75 % at 1 and 2 years		One grade 2 asthenia—met pt
Wulf (2006) [37]	5 (5) primary liver	Estimated life expectancy >6 months	14 cc primary (max 516)	Low-dose group = 28–30 Gy (3–4)	15 months (2–85)	92 % at 1 year	72 % at 1 year	No grade 3 or higher toxicities
	39 (51) mets	No more than 50 % total functional liver receive > 5 Gy Not surgical candidate Extrahepatic disease controlled or treated	9 cc met (max 355)	High-dose group = 12–12.5 Gy (3) or 26 Gy (1)		66 % at 2 years	32 % at 2 years	
Dawson (2006) [38]	79 total 33 HCC 12 IHC 34 Mets	CP Class A; >800 cc non-involved liver	Median 293 cc (2.9–3088 cc)	Median 36.6 (6) Range: 24–57 Gy	NR	74 % (95%CI = 61–83 %)	NR	NR
Hoyer (2006) [28]	65 total pts, of whom 44 treated to liver	Inoperable CRC mets, 1–6 lesions Included SBRT to non-liver sites No chemo within 1 month	Max 6 cm	45 Gy (3)	4.3 years	86 % at 2 years	67 % at 1 year 38 % at 2 years 13 % at 5 years	1 death from liver failure 1 colonic perforation; 2 duodenal ulcers

(continued)

Table 13.4 (continued)

Study (year published)	No. pts (lesions)	Pt population	Tumor size (range)	Dose (no. fractions)	Median follow-up (range)	Local control	OS	Toxicity
Tse (2008) [29]	31 HCC	CP Class A; unresectable; extrahepatic disease okay if bulk of disease in liver	Median = 173 cc (9–1,913 mL)	Median 36 Gy (6)	17.6 months (10.8–39.2)	65 % at 1 year	Median = 13.4 months	7 pts (23 %) progressed to Child–Pugh class B
	10 IHC	More than 800 cc uninvolved liver		Range: 24–54 Gy			[11.7 months (HCC), 15.0 month (IHC)]	
				Every other day			1 year OS = 48 %	
Lee (2009) [30]	68 met pts, including 40 CRC	Unsuitable or refractory to standard treatment	Median = 75.2 cc (1.2–3,090 mL)	Median 41.8 Gy (6)	10.8 months	71 % at 1 year	Median = 17.6 months	7 grade 3–4 acute toxicities
		Life expectancy > 3 months		Range: 27.7–60 Gy (6)			63 % 1 year for CRC mets	1 grade 5 late toxicity (malignant bowel obstruction); 1 grade 4 late toxicity (small bowel obstruction)
		>800 mL uninvolved liver					47 % at 18 months (all histologies)	
		CP Class A						
Rusthoven (2009) [39]	47 (63) mets, including 15 CRC pts	1–3 lesions	Max 6 cm	36–60 Gy	16 months (6–54)	95 % at 1 year	Median 20.5 months	1 grade 3 toxicity (skin/soft tissue)
		Extrahepatic disease permitted if treatable	Median 2.7 cm (0.4–5.8)			92 % at 2 years	30 % at 2 years	
Cardenes (2010) [31]	17 HCC (25)	1–3 lesions	Cumulative diameter 6 cm or less; median vol = 34 cc (8–95)	36–48 Gy (3); later 40 Gy (5) for CTP B	24 months (10–42 months)	100 % at 1 year	58 % at 1 year and 2 years	2 pts radiation-induced liver disease (RILD)
		CP Class A or B; not resection candidates; no progressive or untreated gross extrahepatic disease		1–2 fractions per week				
Goodman (2010) [40]	26 (40) total Inc: 6 CRC mets, 5 IHC, 2 recurrent HCC	1–5 lesions	Max 5 cm	18–30 Gy (1)	17 months (2–55)	77 % at 1 year	Median 28.6 months	No acute or late grade 3 or higher toxicities
		Life expectancy > 6 months					64.3 % at 1 year. 50.4 % at 2 years	
		CP Class A						
		Unresectable or pt-refused resection						
Seo 2010 [41]	38	Inoperable; all received TACE prior to SBRT	<10 cm	33–57 Gy (3–4)		79 %	68 %	Gr 3 skin (1)
						2 years LC = 66 %	2 years = 25 % <42 Gy versus 81 % >42 Gy	

Andolino (2011) [32]	60 HCC	Liver-only disease 36 CTP A 24 CTP B	Median 3.2 cm	CTP A: median 44 Gy (3) CTP B: median 40 Gy (5)	27 months	90 % at 2 years Median TTP 47.8 months	67 % at 2 years For transplant pts, OS 96 % at 2 years	No grade 3 or higher non-heme toxicities 20 % progressed CTP class within 3 months
Rule (2011) [42]	27 (36), almost half CRC	1–5 liver mets >700 mL liver receiving <21 Gy	Median 2.5 cm Range: 0.4–7.8 cm	Dose escalation cohorts: 30 Gy (3) 50 Gy (5) 60 Gy (5)	20 month (4–53)	56 % for 30 Gy, 89 % for 50 Gy, 100 % for 60 Gy at 2 years	50 % for 30 Gy, 67 % for 50 Gy, and 56 % for 60 Gy at 2 years	No grade 4–5 toxicities 1 pt in 50 Gy cohort had grade 3 liver function tests
Bae (2012) [27]	41 (50) CRC mets, of whom 11 (15) treated to liver	1–4 lesions included CRC mets to non-liver sites Radical resection of primary, inoperable, or not amenable to another local treatment	Max 7 cm Median 13 mL sum of individual GTVs (2–123)	Median 48 Gy (3) Range: 45–60 Gy (3)	28 months (6–65)	64 % at 3 years 57 % at 5 years	60 % at 3 years 38 % at 5 years	3 grade 3–4 toxicities (of whom only 1 treated with SBRT to liver)

Complications

The use of radiotherapy to the liver has been limited in the past due to radiation-induced liver disease (RILD). The exact mechanism is unknown although it postulated that endothelial injury or activation of hepatic stellate cells yields fibrin and collagen deposition, resulting in fibrous veno-occlusive disease [139, 140]. Hepatitis B virus status is an independent predictor of RILD development [141] and is therefore anticipated to be a greater factor in HCC patients than those with metastatic disease to the liver.

Clinically, RILD usually develops 2 weeks to 4 months following radiation to the liver, although it has been reported as late as 7 months after radiotherapy. The aspartate transaminase (AST) and alanine transaminase (ALT) levels are moderately elevated with minimal or no increase in bilirubin, but there is an increase of alkaline phophatase to 3–10 times the upper limit of normal. In severe cases, anicteric ascites and hepatomegaly develop. It is usually self-limited and is managed conservatively with medical management, though 10–20 % of patients may die from liver failure, particularly in patients with preexisting hepatic dysfunction such as cirrhosis [142]. In 1991, Emami et al. estimated normal tissue tolerances to radiotherapy based on pooled patient data. The 5 % (TD 5) and 50 % (TD 50) probability of liver failure within 5 years were estimated based on liver volume. In conventional fractionation, the TD5 at 5 years for 1/3, 2/3, and whole liver was estimated to be 50, 35, and 30 Gy, respectively. At 5 years, the TD 50 for 1/3, 2/3, and whole liver was estimated to be 55, 45, and 40 Gy, respectively [143]. More recent studies using different modeling systems have demonstrated that the radiation tolerance of the liver was higher than previously thought. A median dose of 60.75 Gy delivered in twice-daily fractions of 1.5 Gy resulted in 12 %, 9 %, and 1 patient (<1 %) developing grade 3, 4, and 5 toxicities, respectively [144]. Using the Lyman NTCP model, there was an estimated 4 % increased risk of RILD per 1-Gy mean liver dose above 30 Gy [69]. As demonstrated by Dawson et al., the risk of liver injury is related to whether the patient had primary or metastatic liver tumors. The TD 50 for whole liver irradiation was 45.8 Gy for liver metastases versus 39.8 Gy for primary liver tumors [69]. Although this may not be relevant in the patients undergoing extreme hypofractionated regimens as used in SBRT.

Several prospective protocols have been reported and in general have been minimal for patients with metastatic disease as opposed to those with primary disease related to the underlying liver dysfunction. Rusthoven et al. [109], which reported the best outcomes, utilized a three-fraction approach. Patients included in their study include patients with 1–3 metastases with the largest tumor <6 cm. Their most important dosimetric parameter was based on the surgical literature and required the volume of normal liver receiving less than 15 Gy to be at least 700 cc. Following these parameters, no dose-limiting side effects were seen. Rule et al. [136] used a similar parameter keeping the volume of normal liver receiving less than from x Gy to be at least 700 cc, increasing the dose from 15 to 21 Gy based on delivering five fractions as opposed to three. Similarly, Rule et al. did not observe dose-limiting toxicity. Cardenes et al. [131] reported a multi-institutional phase I experience for patients with primary HCC. They included patients with 1–3 tumors with a cumulative tumor size of 6 cm with Child–Pugh scores of A or B. The starting dose was 36 Gy in three fractions with planned escalations of 2 Gy per fraction increments. The dose was escalated to 48 Gy in three fractions without a dose-limiting toxicity for patients with a Child–Pugh score of A. Two with Child–Pugh score B developed grade 3 hepatic toxicity at 14 Gy per fraction and the protocol was amended to a five-fraction approach to 40 Gy which has been tolerable. Mendez Romero et al. [120] described an 18 % incidence of RILD although the patient population was very small. The largest experience reported is from Princess Margaret Hospital which utilized a six-fraction schema and included the largest tumors as well. In their series, no patient developed RILD but they exclude patients with Child–Pugh score B. They did have 5 of 31 patients develop worsening of their Child–Pugh score although 3 of the patients had progressive HCC and had Child–Pugh score A6.

Other potential toxicities include hematologic, fatigue, and nausea that can occur shortly after radiation treatment. The greatest potential late toxicity other than liver is that of the luminal GI organs, which include ulceration, bleeding, and obstruction [24, 129]. Using a maximum dose of 37 Gy in three fractions and 42 Gy in five fractions with additional criteria based on volume of the GI organ at risk, there were no grade 3 or higher acute toxicities and approximately 11 % of patients developed late grade 3 toxicities. One patient died of complications from duodenal perforation 11 months following SABR. Normal tissue constraints used in a Princess Margaret six-fraction phase I study are shown in Table 13.5.

Pancreatic Cancer: The Rationale for SBRT

Pancreatic ductal adenocarcinoma (PDAC) is the fourth leading cause of cancer-related death in the United States.

Table 13.5 SBRT liver study normal tissue permitted tolerances, in six fractions for HCC [38]

Liver	Iso-NTCP model, based on effective liver volume irradiated (for <10 % risk, suggest mean liver dose <16 Gy)
Esophagus	Maximum dose (to 0.5 cc) <30 Gy
Stomach	Maximum dose (to 0.5 cc) <30 Gy
Duodenum	Maximum dose (to 0.5 cc) <30 Gy
Large bowel	Maximum dose (to 0.5 cc) <34 Gy
Kidney	D67% <15 Gy
Spinal cord	Maximum dose <25 Gy

Due to the lack of an early detection method, only 15–20 % of patients can undergo curative resection at the time of diagnosis [81]. Among resectable patients who receive postoperative radiotherapy, the median OS is approximately 20 months but these patients do not reflect the 25 % of patients with resectable disease who have radiographically occult metastases and do not undergo resection [145, 146]. For patients with resectable PDAC who receive neoadjuvant therapy and do not undergo laparoscopy prior to therapy, a median OS of 12–23 months could be expected [147, 148]. Unfortunately, even in the initially resectable population and despite curative surgery followed by adjuvant chemotherapy and/or chemoradiation, the risk of local and distant recurrence remains high at 37 % and 75 %, respectively, and tumor recurrence typically within 12 months after surgery [145, 146]. This suggests the presence of disseminated cancer cells at the time of surgery. For this reason, the role of conventionally fractionated radiation therapy in addition to systemic chemotherapy alone has been questioned due to the predominance of distant failures. Recently, improved systemic options have been developed which may again alter the patterns of failure such that local therapy may become more important again.

Early Experience in Pancreas

While the experience with SBRT for pancreatic malignancies is less than other sites, the rationale for using SBRT in PDAC is quite similar to that in early lung cancer. The benefits of hypofractionated RT allow for greater tumor kill due to radiobiologic superiority and allow for less interruption with more effective systemic chemotherapy regimens. Since hypofractionated courses of therapy can be delivered in 1–5 treatments, generally in less than 1 week. This can make it easy to incorporate into systemic therapy optimizing local control without interfering with distant disease control since systemic therapy will not need to be altered as in more conventionally fractionated radiotherapy. Given its location, surrounded by extremely radiosensitive critical structures such as the small bowel, stomach, and liver, SBRT for PDAC represents a unique challenge. The small bowel has been known to be susceptible to radiation-induced necrosis, bleeding, and stenosis with conventional fractionation doses above 50 Gy and the additional biologically equivalent dose can pose a significant threat to the integrity of these critical structures. In addition, accounting for pancreatic motion often results in large ITV margins that may result in large volumes of small bowel being treated.

Compared to the available clinical data with SBRT for malignancies of the lung and liver, only a few prospective studies have been published for PDAC similar to literature a decade ago for lung cancer [129, 149–151]. Similar to the early experience in lung cancer, a wide range of doses and treatment delivery tools have been used with common result, very encouraging local control. In the absence of prospective studies, single institutional experiences have played a major role in our understanding of the role for SBRT in pancreatic cancer. These can be divided into experiences in the palliative setting, where most of the prevalent data exists, and those in the neoadjuvant setting.

Experience with SBRT as a Definitive (Including Palliative) Treatment

The initial reports with the use of SBRT in pancreatic cancer came from Koong and colleagues [149]. In a single institution phase I dose escalation study from Stanford University, 15 patients with locally advanced pancreatic cancer and ECOG performance status ≤ 2 were treated with a single dose of 15 (3 patients), 20 (5 patients), or 25 Gy (7 patients) to the primary tumor alone with no specific targeting of the elective lymph nodes. Treatment planning was performed on thin-cut, contrast-enhanced CT images, and radiation was delivered using the CyberKnife® system (Accuray Inc., Sunnyvale, CA). All patients had three to five fiducial markers implanted in the tumor to facilitate image guidance during SBRT. Patients were treated with orthogonal X-rays prior to treatment to ensure appropriate positioning of the fiducial markers, with the pancreas immobilized in voluntary breath hold. The treatment time ranged from 3 to 6 h. The proximal duodenum was not allowed to receive more than 50 % of the prescribed dose though the prescription isodose line was variable from 64 to 85 %. Of the 15 treated patients, only 2 had received any prior RT as part of their therapy. Despite treating patients with essentially advanced unresectable tumors, 84 % local control was seen at 1 year with no acute grade 3 or higher toxicity despite use of a very large single dose [148]. In fact, local control in the patients receiving 25 Gy was 100 % (6 patients with imaging follow-up) though they all failed distantly. Median survival for the entire group of patients was 11 months. The most frequently seen adverse events were grade 2 nausea, diarrhea, and abdominal pain in 5 patients. The same group subsequently performed a dose escalation study using SBRT as a planned boost following conventionally fractionated RT (1.8 Gy/fraction) to the primary and regional lymph nodes with 5-fluorouracil [151]. Based on the safety demonstrated in their phase I results, a single dose of 25 Gy was administered for the boost dose to the tumor alone [152]. Overall, the regimen was well tolerated with grade 3 acute GI toxicity noted in 2 patients who subsequently went on to develop symptomatic duodenal ulceration. Median survival was 33 weeks and median progression-free survival was 17.5 weeks. All but one of the 16 enrolled patients were controlled locally; however, distant disease manifested in all of them eventually. Additionally from the same group, Chang et al. [153] published a retrospective

experience of 77 patients treated with 25 Gy to the 95 % isodose line covering the PTV. In this rather heterogeneous group of patients (73 % unresectable, 5 % medically inoperable, 3 % marginally resectable, and 19 % metastatic), median survival from date of diagnosis was 11.4 months. Once again, grade 3 or higher acute toxicities were low with only one patient experiencing a gastric ulcer. Late toxicities (≥grade 3) included gastric ulceration in 3, duodenal stricture in 1, and biliary stricture in 2 patients, respectively. Only one patient experienced a grade 4 toxicity consisting of small bowel perforation. Murphy et al. [154] reported dosimetric parameters that predicted grade 2 and higher duodenal toxicity which was seen in 11 % and 29 % of their patients at 6 and 12 months, respectively. Based on their data from delivering SBRT in a single fraction, the absolute volumes of the duodenum receiving 10, 15, 20, and 25 Gy were all significant predictors of increased toxicity. The absolute volumes for each parameter were 16, 9.1, 3.3, and 0.21 cc, respectively. In addition, when the maximum dose was >23 Gy, the grade 2–4 duodenal toxicity rate was 45 % compared to 12 % when the dose was <23 Gy.

A recent retrospective publication of the University of Pittsburgh experience by Rwigema and coworkers [155] also suggests a relatively safe profile of SBRT for unresectable pancreas. In their 71 patient experience of patients treated on either the CyberKnife or the Trilogy linear accelerator system (Varian Medical, Palo Alto, CA), patients received a single fraction of between 18 and 25 Gy. Prescription was to the 80 % isodose shell when using the CyberKnife and to the 89 % isodose shell when using the linear accelerator-based system. Median survival for the entire group was 10.3 months, and local failure was seen in 35 % of the patients. Dosimetric correlatives suggested that local control was improved with doses above 24 Gy being administered. Toxicity was once again low with only 4 % of patients reporting ≥ grade 3 GI toxicity.

Mahadevan and coworkers [151] adopted a slightly less aggressive approach using three fractions of SBRT sandwiched between cycles 3 and 4 of gemcitabine also using the CyberKnife® platform. Local control was 85 % in their 47 patients with late grade 3 and higher toxicities related to radiotherapy seen in only 9 %. For disease abutting a large area of the duodenal loop, the prescribed dose was 24 Gy in three fractions while disease with minimal contact in this region was treated to 30 Gy in three fractions. PDAC with no involvement of the duodenal c-loop was treated to 12 Gy in three fractions for a total of 36 Gy on this study. Median progression-free survival for these patients was 15 months and the median overall survival was 20 months. In addition, the sandwich approach with the initial systemic treatment allowed patients with early metastases to be excluded similar to the recommendations from the GERCOR study [156] and thereby assuring local treatment only in appropriate patients. These and several other reports have demonstrated that SBRT for pancreas is associated with excellent local control, with toxicity that seems similar when delivered with accurate precision and careful planning.

Contrasting with the high level of safety and efficacy from these reports, a prospective phase II trial [129] was conducted in Denmark for patients with biopsy-proven adenocarcinomas of the pancreas that were N0 and less than 6 cm in maximum dimension. They prescribed 45 Gy over three fractions with the dose prescribed to the ICRU reference point such that 95 % of the prescribed dose was delivered to the CTV and 67 % of the prescribed dose was delivered to the PTV. The CTV was defined as the GTV plus the surrounding edema, while the PTV was defined as the CTV plus 5 mm in the axial direction and 1 cm in the cranial–caudal direction. Motion management was controlled by two different methods using abdominal compression or a "slow" CT simulation. IGRT was performed using portal imaging. Their findings were concerning, with patients having one or more grade 2 side effects in 64 % of the patients by 2 weeks. Despite the use of prophylactic ondansetron and pantoprazole for 4 weeks, acute toxicity at 14 days after therapy was pronounced, with worsening of nausea and pain that resolved in 8 of 12 patients 3 months after SBRT. Progression to grade 2 or higher toxicity occurs in 79 % of patients and the overall performance status is significantly deteriorating. In addition some of the patients were lost to follow-up or deteriorated quickly with only 14 of the original 22 patients making it to 2 months after treatment and 4 patients with 6 months of follow-up. In 5 patients there was evidence of severe mucositis (2), ulceration (2), and ulcus-perforation of the stomach (1). The actuarial local failure rate was substantially higher than other experiences at 43 %. In addition, median survival and 1-year survival were also lower at 5.7 months and 5 %, respectively. There were differences in their treatment approach that may explain the dismal outcomes. Treatment was administered using a linear accelerator-based approach using abdominal compression and a stereotactic body frame, and was targeted to the primary tumor and surrounding edema. The CTV (created by expanding the tumor plus edema by 1 cm in the sup-inf direction and 5 mm axially) was targeted to receive >95 % of the prescribed dose while the PTV (including the motion component) received at least 67 %. Therefore, these volumes were significantly larger with parts of the duodenum and stomach (included in the PTV) receiving up to 67 % of the prescribed dose. Abdominal compression may cause patient discomfort making longer treatments less reproducible which can increase the likelihood of marginal failures that could increase local failures and increase dose to critical surrounding normal tissues inadvertently increasing side effects. Also of note, the prospective nature of this trial mandated strict posttreatment biopsy protocols and may also account for the larger percentage of patients identified with

local failure when contrasted with those assessed by imaging-based RECIST criteria in other studies. Therefore, this dosing scheme and planning methodology may not be safely deliverable to the upper abdomen. Although, most investigators believe lower dose SBRT is more reasonable for palliation.

Experience in the Borderline Resectable Setting with a Goal to Achieve Resectability

More recently, Schellenberg et al. [152] from Stanford reported two studies, using 3 weekly doses of full dose (1,000 mg/m^2) of gemcitabine (days 1, 8, 15) followed 2 weeks later by a single dose of 25 Gy administration to the primary pancreas tumor on day 29. The first 16 patients underwent SBRT using the CyberKnife platform with the dose prescribed to the 95 % isodose shell. Subsequently, patients went on to receive one further cycle of gemcitabine. While none of the patients made it to resectability, all 16 enrolled patients were able to complete treatment, and 13/16 exhibited local control with minimal acute toxicity. Median and 1-year overall survival were 11.4 months and 50 %, respectively. Despite the initial minimal acute toxicity profile, late toxicities included five grade 2, one grade 3, and one grade 4 duodenal complications. Correlation of the toxicity profile with treatment isodose lines did not seem to suggest correlation of duodenal toxicity with a particular minimal level of dose received. The second phase 2 study used the sandwich approach once again using 25 Gy delivered following 3 weekly doses of gemcitabine. However, treatment on this study was delivered using a linear accelerator and 4D CT and PET scan were used to delineate the target, and fiducials were used to provide fluoroscopic target acquisition. A 9-beam arrangement was optimized to deliver dose to the 95 % isodose line. Median survival was 11.8 months and the local failure rate was 5 %. Late grade 2 toxicity was seen in 20 % of the patients and late grade 3 toxicity was only seen in 1 (5 %) patient. Subsequently, gemcitabine was administered till disease progression. Overall, this regimen did support the limited use of SBRT in patients treated with gemcitabine and allowed for a sandwich approach which may be important as a strategy to address early treatment with systemic therapy prior to local treatment.

An Italian phase I study by Polistina and coworkers [150] treated 23 patients with a 10 Gy×3 fractionation scheme sandwiched between systemic dosing cycles of gemcitabine. A complete (imaging based) response was seen in 9 % of patients, along with a partial response in 61 % of patients and no progression in 13 % of patients. Median survival was 10.6 months and no reported ≥grade 2 acute or late toxicities were seen with local progression being seen in only 17 % of patients. Furthermore, selected patients getting gemcitabine and SBRT were still able to proceed to surgical resection, an important observation when considering SBRT as a component of future neoadjuvant strategies.

Future Directions

Recently, systemic therapy for pancreatic cancer has improved significantly. Similar to breast cancer and lung cancer, improving systemic control may have a major impact on increasing local failures due to the predominant presence of residual disease subsequently improved local control will become vital. The PRODIGE 4/ACCORD 11 study by Conroy and coworkers [157, 158] demonstrated a significant improvement in median survival in metastatic PDAC increasing from 6.9 to 10.5 months with 5-fluorouracil, leucovorin, oxaliplatin, and irinotecan or FOLFIRINOX. This regimen is now being investigated in all settings of this disease. Investigators are currently testing the combination of this regimen with SBRT to the involved disease.

Treatment Planning Considerations

The proximity of the pancreas to extremely radiosensitive critical structures such as the duodenum, liver, kidneys, and stomach, in addition to its association with respiratory and peristaltic motion, presents a unique challenge in choosing appropriate modalities for immobilization and for motion accounting. In addition, it is often difficult to delineate the tumor based on CT imaging. In the absence of well-endorsed guidelines, a commonsense approach combining the experiences of the currently available literature in this field suggests that the use of multiphasic thin (ideally 2.5 mm) CT slices in addition to a four-dimensional CT scan should be used at a minimum. In experienced centers, the use of fiducial markers can be an invaluable tool in daily setup verification or motion tracking in the case of treatment with the CyberKnife. In all cases, the use of oral contrast to delineate the stomach and small bowel should be considered. In addition, intravenous contrast should be used as long as renal function permits.

Conclusion

SBRT is an exciting new field of radiation oncology that brings together many of the technological advancements that have occurred recently in radiation oncology. SBRT is not specific to one planning system or delivery method but requires utilization of high-quality imaging for target definition, immobilization, high-precision planning, and delivery and image guidance. Using these technological advancements, potent radiobiological doses can be delivered in convenient fractionation schemes, generally ranging from one to five fractions.

Preliminary data suggest that SBRT can be delivered safely with a high likelihood of local control and an acceptable safety profile for most sites. Clinical outcomes are expected to be improved even further if SBRT can be combined with other treatments such as surgery and chemotherapy, and future research efforts should include determining optimal combinations of SBRT with other therapeutic modalities.

The high doses and highly conformal SBRT plans are more prone to error introduced by geometric or dosimetry uncertainties. Such errors could lead to permanent and serious late normal tissue toxicity, and thus caution is required when SBRT is used clinically. Serious late toxicities have been reported after SBRT, including radiation-induced liver injury and gastrointestinal bleeding. As we gain increased experience with SBRT, the partial volume tolerances to hypofractionated heterogeneous radiation delivered to normal tissues should be able to be better defined. Optimal fractionations, methods of guidance, and clinical applications of SBRT are not well established, and clinical trials continue to be required in this field, especially in North America.

References

1. Kavanagh B, Timmerman R. Stereotactic body radiation therapy. Philadelphia: Lippincott Williams & Wilkins; 2005.
2. Potters L, Steinberg M, Rose C, Timmerman R, Ryu S, Hevezi JM, et al. American Society for Therapeutic Radiology and Oncology and American College of Radiology practice guideline for the performance of stereotactic body radiation therapy. Int J Radiat Oncol Biol Phys. 2004;60(4):1026–32.
3. Hamilton AJ, Lulu BA. A prototype device for linear accelerator-based extracranial radiosurgery. Acta Neurochir Suppl. 1995;63:40–3.
4. Lax I, Blomgren H, Naslund I, Svanstrom R. Stereotactic radiotherapy of malignancies in the abdomen. Methodological aspects. Acta Oncol. 1994;33(6):677–83.
5. Blomgren H, Lax I, Naslund I, Svanstrom R. Stereotactic high dose fraction radiation therapy of extracranial tumors using an accelerator. Clinical experience of the first thirty-one patients. Acta Oncol. 1995;34(6):861–70.
6. Timmerman R, Papiez L, McGarry R, Likes L, DesRosiers C, Frost S, et al. Extracranial stereotactic radioablation: results of a phase I study in medically inoperable stage I non-small cell lung cancer. Chest. 2003;124(5):1946–55.
7. McGarry RC, Papiez L, Williams M, Whitford T, Timmerman RD. Stereotactic body radiation therapy of early-stage non-small-cell lung carcinoma: phase I study. Int J Radiat Oncol Biol Phys. 2005;63(4):1010–5.
8. Timmerman R, McGarry R, Yiannoutsos C, Papiez L, Tudor K, DeLuca J, et al. Excessive toxicity when treating central tumors in a phase II study of stereotactic body radiation therapy for medically inoperable early-stage lung cancer. J Clin Oncol. 2006;24(30):4833–9.
9. Fakiris AJ, McGarry RC, Yiannoutsos CT, Papiez L, Williams M, Henderson MA, et al. Stereotactic body radiation therapy for early-stage non-small-cell lung carcinoma: four-year results of a prospective phase II study. Int J Radiat Oncol Biol Phys. 2009;75(3):677–82.
10. Timmerman R, Paulus R, Galvin J, Michalski J, Straube W, Bradley J, et al. Stereotactic body radiation therapy for inoperable early stage lung cancer. JAMA. 2010;303(11):1070–6.
11. Timmerman RD. Surgery versus stereotactic body radiation therapy for early-stage lung cancer: who's down for the count? J Clin Oncol. 2010;28(6):907–9.
12. Mehta M, Scrimger R, Mackie R, Paliwal B, Chappell R, Fowler J. A new approach to dose escalation in non-small-cell lung cancer. Int J Radiat Oncol Biol Phys. 2001;49(1):23–33.
13. Fowler JF. Linear quadratics is alive and well: in regard to Park et al. (Int J Radiat Oncol Biol Phys 2008;70:847–852). Int J Radiat Oncol Biol Phys. 2008;72(3):957; author reply 8.
14. Fowler JF. Review: total doses in fractionated radiotherapy—implications of new radiobiological data. Int J Radiat Biol Relat Stud Phys Chem Med. 1984;46(2):103–20.
15. Hayman JA, Martel MK, Ten Haken RK, Normolle DP, Todd III RF, Littles JF, et al. Dose escalation in non-small-cell lung cancer using three-dimensional conformal radiation therapy: update of a phase I trial. J Clin Oncol. 2001;19(1):127–36.
16. Narayan S, Henning GT, Ten Haken RK, Sullivan MA, Martel MK, Hayman JA. Results following treatment to doses of 92.4 or 102.9 Gy on a phase I dose escalation study for non-small cell lung cancer. Lung Cancer. 2004;44(1):79–88.
17. Wulf J, Hadinger U, Oppitz U, Thiele W, Ness-Dourdoumas R, Flentje M. Stereotactic radiotherapy of targets in the lung and liver. Strahlenther Onkol. 2001;177(12):645–55.
18. Park C, Papiez L, Zhang S, Story M, Timmerman RD. Universal survival curve and single fraction equivalent dose: useful tools in understanding potency of ablative radiotherapy. Int J Radiat Oncol Biol Phys. 2008;70(3):847–52.
19. Fuks Z, Kolesnick R. Engaging the vascular component of the tumor response. Cancer Cell. 2005;8(2):89–91.
20. Grills IS, Mangona VS, Welsh R, Chmielewski G, McInerney E, Martin S, et al. Outcomes after stereotactic lung radiotherapy or wedge resection for stage I non-small-cell lung cancer. J Clin Oncol. 2010;28(6):928–35.
21. Galon J, Costes A, Sanchez-Cabo F, Kirilovsky A, Mlecnik B, Lagorce-Pages C, et al. Type, density, and location of immune cells within human colorectal tumors predict clinical outcome. Science. 2006;313(5795):1960–4.
22. Franzke A, Buer J, Probst-Kepper M, Lindig C, Framzle M, Schrader AJ, et al. HLA phenotype and cytokine-induced tumor control in advanced renal cell cancer. Cancer Biother Radiopharm. 2001;16(5):401–9.
23. Gray WC, Chretien PB, Suter CM, Revie DR, Tomazic VT, Blanchard CL, et al. Effects of radiation therapy on T-lymphocyte subpopulations in patients with head and neck cancer. Otolaryngol Head Neck Surg. 1985;93(5):650–60.
24. Lee Y, Auh SL, Wang Y, Burnette B, Wang Y, Meng Y, et al. Therapeutic effects of ablative radiation on local tumor require CD8+ T cells: changing strategies for cancer treatment. Blood. 2009;114(3):589–95.
25. Mahmoud SM, Lee AH, Paish EC, Macmillan RD, Ellis IO, Green AR. The prognostic significance of B lymphocytes in invasive carcinoma of the breast. Breast Cancer Res Treat. 2012;132:545–53.
26. Mahmoud SM, Paish EC, Powe DG, Macmillan RD, Grainge MJ, Lee AH, et al. Tumor-infiltrating CD8+ lymphocytes predict clinical outcome in breast cancer. J Clin Oncol. 2011;29(15):1949–55.
27. Denkert C, Loibl S, Noske A, Roller M, Muller BM, Komor M, et al. Tumor-associated lymphocytes as an independent predictor of response to neoadjuvant chemotherapy in breast cancer. J Clin Oncol. 2010;28(1):105–13.
28. Paulson KG, Iyer JG, Tegeder AR, Thibodeau R, Schelter J, Koba S, et al. Transcriptome-wide studies of merkel cell carcinoma and validation of intratumoral CD8+ lymphocyte invasion as an independent predictor of survival. J Clin Oncol. 2011;29(12):1539–46.
29. Postow MA, Callahan MK, Barker CA, Yamada Y, Yuan J, Kitano S, et al. Immunologic correlates of the abscopal effect in a patient with melanoma. N Engl J Med. 2012;366(10):925–31.
30. Takeda T, Takeda A, Kunieda E, Ishizaka A, Takemasa K, Shimada K, et al. Radiation injury after hypofractionated stereotactic radiotherapy for peripheral small lung tumors: serial changes on CT. AJR Am J Roentgenol. 2004;182(5):1123–8.

31. Kimura T, Matsuura K, Murakami Y, Hashimoto Y, Kenjo M, Kaneyasu Y, et al. CT appearance of radiation injury of the lung and clinical symptoms after stereotactic body radiation therapy (SBRT) for lung cancers: are patients with pulmonary emphysema also candidates for SBRT for lung cancers? Int J Radiat Oncol Biol Phys. 2006;66(2):483–91.
32. Scott WJ, Schwabe JL, Gupta NC, Dewan NA, Reeb SD, Sugimoto JT. Positron emission tomography of lung tumors and mediastinal lymph nodes using [18F]fluorodeoxyglucose. The members of the PET-Lung Tumor Study Group. Ann Thorac Surg. 1994;58(3):698–703.
33. Shim SS, Lee KS, Kim BT, Chung MJ, Lee EJ, Han J, et al. Non-small cell lung cancer: prospective comparison of integrated FDG PET/CT and CT alone for preoperative staging. Radiology. 2005;236(3):1011–9.
34. Magnani P, Carretta A, Rizzo G, Fazio F, Vanzulli A, Lucignani G, et al. FDG/PET and spiral CT image fusion for mediastinal lymph node assessment of non-small cell lung cancer patients. J Cardiovasc Surg (Torino). 1999;40(5):741–8.
35. Decoster L, Schallier D, Everaert H, Nieboer K, Meysman M, Neyns B, et al. Complete metabolic tumour response, assessed by 18-fluorodeoxyglucose positron emission tomography (18FDG-PET), after induction chemotherapy predicts a favourable outcome in patients with locally advanced non-small cell lung cancer (NSCLC). Lung Cancer. 2008;62(1):55–61.
36. Vansteenkiste JF, Mortelmans LA. FDG-PET in the locoregional lymph node staging of non-small cell lung cancer. A comprehensive review of the Leuven Lung Cancer Group experience. Clin Positron Imaging. 1999;2(4):223–31.
37. Higashi T, Saga T, Nakamoto Y, Ishimori T, Mamede MH, Wada M, et al. Relationship between retention index in dual-phase (18) F-FDG PET, and hexokinase-II and glucose transporter-1 expression in pancreatic cancer. J Nucl Med. 2002;43(2):173–80.
38. Cohen RJ, Sharma NK, Yu JQ, et al. A phase I radiation dose escalation trial of stereotactic body radiotherapy for malignant lung tumors. J Biomed Sci Eng. 2010;3(4):351–8.
39. Sharma NK, Ruth K, Konski AA, et al. Low morbidity and excellent local control using image guided stereotactic body radiotherapy (IGSBRT) for lung tumors. Int J Radiat Oncol Biol Phys. 2008;72(1):S454.
40. Husain ZA, Sharma NK, Hanlon AL, Buyyounouski MK, Mirmiran A, Dhople AA, Turaka A, Yu M, Chen W, Feigenberg SJ. Low pretreatment PET SUV predicts for increased local failure following stereotactic body radiation therapy for lung cancer. Int J Radiat Oncol Biol Phys. 2010;78(3):S525.
41. Hoopes DJ, Tann M, Fletcher JW, Forquer JA, Lin PF, Lo SS, et al. FDG-PET and stereotactic body radiotherapy (SBRT) for stage I non-small-cell lung cancer. Lung Cancer. 2007;56(2):229–34.
42. Sovik A, Malinen E, Skogmo HK, Bentzen SM, Bruland OS, Olsen DR. Radiotherapy adapted to spatial and temporal variability in tumor hypoxia. Int J Radiat Oncol Biol Phys. 2007;68(5):1496–504.
43. Ishimori T, Saga T, Nagata Y, Nakamoto Y, Higashi T, Mamede M, et al. 18F-FDG and 11C-methionine PET for evaluation of treatment response of lung cancer after stereotactic radiotherapy. Ann Nucl Med. 2004;18(8):669–74.
44. Direcks WG, Berndsen SC, Proost N, Peters GJ, Balzarini J, Spreeuwenberg MD, et al. [18F]FDG and [18F]FLT uptake in human breast cancer cells in relation to the effects of chemotherapy: an in vitro study. Br J Cancer. 2008;99(3):481–7.
45. van Luijk P, Bijl HP, Konings AW, van der Kogel AJ, Schippers JM. Data on dose-volume effects in the rat spinal cord do not support existing NTCP models. Int J Radiat Oncol Biol Phys. 2005;61(3):892–900.
46. Dawson LA, Eccles C, Craig T. Individualized image guided iso-NTCP based liver cancer SBRT. Acta Oncol. 2006;45(7):856–64.
47. Dawson LA, Litzenberg DW, Brock KK, Sanda M, Sullivan M, Sandler HM, et al. A comparison of ventilatory prostate movement in four treatment positions. Int J Radiat Oncol Biol Phys. 2000;48(2):319–23.
48. Malone S, Crook JM, Kendal WS, Szanto J. Respiratory-induced prostate motion: quantification and characterization. Int J Radiat Oncol Biol Phys. 2000;48(1):105–9.
49. Yenice KM, Lovelock DM, Hunt MA, Lutz WR, Fournier-Bidoz N, Hua CH, et al. CT image-guided intensity-modulated therapy for paraspinal tumors using stereotactic immobilization. Int J Radiat Oncol Biol Phys. 2003;55(3):583–93.
50. Meeks SL, Buatti JM, Bouchet LG, Bova FJ, Ryken TC, Pennington EC, et al. Ultrasound-guided extracranial radiosurgery: technique and application. Int J Radiat Oncol Biol Phys. 2003;55(4):1092–101.
51. Wulf J, Hadinger U, Oppitz U, Olshausen B, Flentje M. Stereotactic radiotherapy of extracranial targets: CT-simulation and accuracy of treatment in the stereotactic body frame. Radiother Oncol. 2000;57(2):225–36.
52. Lohr F, Debus J, Frank C, Herfarth K, Pastyr O, Rhein B, et al. Noninvasive patient fixation for extracranial stereotactic radiotherapy. Int J Radiat Oncol Biol Phys. 1999;45(2):521–7.
53. Booth JT, Zavgorodni SF. Set-up error & organ motion uncertainty: a review. Australas Phys Eng Sci Med. 1999;22(2):29–47.
54. Dawson LA, Brock KK, Kazanjian S, Fitch D, McGinn CJ, Lawrence TS, et al. The reproducibility of organ position using active breathing control (ABC) during liver radiotherapy. Int J Radiat Oncol Biol Phys. 2001;51(5):1410–21.
55. Eccles C, Brock KK, Bissonnette JP, Hawkins M, Dawson LA. Reproducibility of liver position using active breathing coordinator for liver cancer radiotherapy. Int J Radiat Oncol Biol Phys. 2006;64(3):751–9.
56. Sonke JJ, Zijp L, Remeijer P, van Herk M. Respiratory correlated cone beam CT. Med Phys. 2005;32(4):1176–86.
57. Claude L, Arpin D, Servois V, Ayadi M, Dussart S, Ferlay C, et al. Acute radiation pneumonitis in non-small cell lung cancer: is respiratory-gated control useful? Results of a French Prospective Randomized Study. Int J Radiat Oncol Biol Phys. 2012;84(3):S175.
58. Shirato H, Shimizu S, Kitamura K, Nishioka T, Kagei K, Hashimoto S, et al. Four-dimensional treatment planning and fluoroscopic real-time tumor tracking radiotherapy for moving tumor. Int J Radiat Oncol Biol Phys. 2000;48(2):435–42.
59. Benedict SH, Yenice KM, Followill D, Galvin JM, Hinson W, Kavanagh B, et al. Stereotactic body radiation therapy: the report of AAPM Task Group 101. Med Phys. 2010;37(8):4078–101.
60. Balter JM, Lam KL, McGinn CJ, Lawrence TS, Ten Haken RK. Improvement of CT-based treatment-planning models of abdominal targets using static exhale imaging. Int J Radiat Oncol Biol Phys. 1998;41(4):939–43.
61. Arvidson NB, Mehta MP, Tome WA. Dose coverage beyond the gross tumor volume for various stereotactic body radiotherapy planning techniques reporting similar control rates for stage I non-small-cell lung cancer. Int J Radiat Oncol Biol Phys. 2008;72(5):1597–603.
62. van Herk M, Remeijer P, Rasch C, Lebesque JV. The probability of correct target dosage: dose-population histograms for deriving treatment margins in radiotherapy. Int J Radiat Oncol Biol Phys. 2000;47(4):1121–35.
63. van Herk M, Remeijer P, Lebesque JV. Inclusion of geometric uncertainties in treatment plan evaluation. Int J Radiat Oncol Biol Phys. 2002;52(5):1407–22.
64. Jin L, Wang L, Li J, Luo W, Feigenberg SJ, Ma CM. Investigation of optimal beam margins for stereotactic radiotherapy of lung-cancer

using Monte Carlo dose calculations. Phys Med Biol. 2007;52(12):3549–61.
65. Kavanagh BD, Timmerman RD, Benedict SH, Wu Q, Schefter TE, Stuhr K, et al. How should we describe the radiobiologic effect of extracranial stereotactic radiosurgery: equivalent uniform dose or tumor control probability? Med Phys. 2003;30(3):321–4.
66. DesRosiers PM, Moskvin VP, DesRosiers CM, Timmerman RD, Randall ME, Papiez LS. Lung cancer radiation therapy: Monte Carlo investigation of "under dose" by high energy photons. Technol Cancer Res Treat. 2004;3(3):289–94.
67. Xiao Y, Papiez L, Paulus R, Timmerman R, Straube WL, Bosch WR, et al. Dosimetric evaluation of heterogeneity corrections for RTOG 0236: stereotactic body radiotherapy of inoperable stage I-II non-small-cell lung cancer. Int J Radiat Oncol Biol Phys. 2009;73(4):1235–42.
68. Dawson LA, Eccles C, Bissonnette JP, Brock KK. Accuracy of daily image guidance for hypofractionated liver radiotherapy with active breathing control. Int J Radiat Oncol Biol Phys. 2005;62(4):1247–52.
69. Balter JM, Brock KK, Litzenberg DW, McShan DL, Lawrence TS, Ten Haken R, et al. Daily targeting of intrahepatic tumors for radiotherapy. Int J Radiat Oncol Biol Phys. 2002;52(1):266–71.
70. Uematsu M, Sonderegger M, Shioda A, Tahara K, Fukui T, Hama Y, et al. Daily positioning accuracy of frameless stereotactic radiation therapy with a fusion of computed tomography and linear accelerator (focal) unit: evaluation of z-axis with a z-marker. Radiother Oncol. 1999;50(3):337–9.
71. Court L, Rosen I, Mohan R, Dong L. Evaluation of mechanical precision and alignment uncertainties for an integrated CT/LINAC system. Med Phys. 2003;30(6):1198–210.
72. Kuriyama K, Onishi H, Sano N, Komiyama T, Aikawa Y, Tateda Y, et al. A new irradiation unit constructed of self-moving gantry-CT and linac. Int J Radiat Oncol Biol Phys. 2003;55(2):428–35.
73. Onishi H, Kuriyama K, Komiyama T, Tanaka S, Sano N, Aikawa Y, et al. A new irradiation system for lung cancer combining linear accelerator, computed tomography, patient self-breath-holding, and patient-directed beam-control without respiratory monitoring devices. Int J Radiat Oncol Biol Phys. 2003;56(1):14–20.
74. Jaffray DA. Emergent technologies for 3-dimensional image-guided radiation delivery. Semin Radiat Oncol. 2005;15(3):208–16.
75. Cho Y, Moseley DJ, Siewerdsen JH, Jaffray DA. Accurate technique for complete geometric calibration of cone-beam computed tomography systems. Med Phys. 2005;32(4):968–83.
76. Simpson RG, Chen CT, Grubbs EA, Swindell W. A 4-MV CT scanner for radiation therapy: the prototype system. Med Phys. 1982;9(4):574–9.
77. Swindell W, Simpson RG, Oleson JR, Chen CT, Grubbs EA. Computed tomography with a linear accelerator with radiotherapy applications. Med Phys. 1983;10(4):416–20.
78. Nakagawa K, Aoki Y, Tago M, Terahara A, Ohtomo K. Megavoltage CT-assisted stereotactic radiosurgery for thoracic tumors: original research in the treatment of thoracic neoplasms. Int J Radiat Oncol Biol Phys. 2000;48(2):449–57.
79. Pouliot J, Bani-Hashemi A, Chen J, Svatos M, Ghelmansarai F, Mitschke M, et al. Low-dose megavoltage cone-beam CT for radiation therapy. Int J Radiat Oncol Biol Phys. 2005;61(2):552–60.
80. Klein EE, Hanley J, Bayouth J, Yin FF, Simon W, Dresser S, et al. Task Group 142 report: quality assurance of medical accelerators. Med Phys. 2009;36(9):4197–212.
81. Jemal A, Siegel R, Ward E, Hao Y, Xu J, Thun MJ. Cancer statistics, 2009. CA Cancer J Clin. 2009;59(4):225–49.
82. Mountain CF. Revisions in the International System for Staging Lung Cancer. Chest. 1997;111(6):1710–7.
83. McGarry RC, Song G, des Rosiers P, Timmerman R. Observation-only management of early stage, medically inoperable lung cancer: poor outcome. Chest. 2002;121(4):1155–8.
84. Stephans KL, Djemil T, Reddy CA, Gajdos SM, Kolar M, Mason D, et al. A comparison of two stereotactic body radiation fractionation schedules for medically inoperable stage I non-small cell lung cancer: the Cleveland Clinic experience. J Thorac Oncol. 2009;4(8):976–82.
85. Shapiro R, Forquer JA, Henderson MA, Brabham JG, Barriger RB, Andolino DL, Johnstone PAS, Fakiris AJ. Central Tumors in Node Negative Early-stage Non-small Cell Lung Cancer (NSCLC): survival and toxicity outcomes following Stereotactic Body Radiation Therapy (SBRT). Int J Radiat Oncol Biol Phys. 2009;75(3):S457.
86. Bradley JD, Robinson C, Parikh P, Bien-Willner L, DeWees T, Gao F. Prospective phase i dose escalation results of SBRT for centrally-located stage I NSCLC. Int J Radiat Oncol Biol Phys. 2011;81(2):S79.
87. Stephans KL, Djemil T, Reddy CA, Gajdos SM, Kolar M, Machuzak M, et al. Comprehensive analysis of pulmonary function Test (PFT) changes after stereotactic body radiotherapy (SBRT) for stage I lung cancer in medically inoperable patients. J Thorac Oncol. 2009;4(7):838–44.
88. Buyyounouski MK, Balter P, Lewis B, D'Ambrosio DJ, Dilling TJ, Miller RC, et al. Stereotactic body radiotherapy for early-stage non-small-cell lung cancer: report of the ASTRO Emerging Technology Committee. Int J Radiat Oncol Biol Phys. 2010;78(1):3–10.
89. Guckenberger M, Kestin LL, Hope AJ, Belderbos J, Werner-Wasik M, Yan D, et al. Is there a lower limit of pretreatment pulmonary function for safe and effective stereotactic body radiotherapy for early-stage non-small cell lung cancer? J Thorac Oncol. 2012;7(3):542–51.
90. Onishi H, Marino K, Terahara A, Kokubo M, Onimaru R, Shioyama Y, Matsuo Y, Kozuka T, Ishikura S, Hiraoka M. Case series study of 26 patients who developed fatal radiation pneumonitis (RP) after stereotactic body radiotherapy for lung cancer. Int J Radiat Oncol Biol Phys. 2009;75(3):S62.
91. Hughes LL, Wang M, Page DL, Gray R, Solin LJ, Davidson NE, et al. Local excision alone without irradiation for ductal carcinoma in situ of the breast: a trial of the Eastern Cooperative Oncology Group. J Clin Oncol. 2009;27(32):5319–24.
92. Wambaka MA, Matsuo Y, Shibuya K, Ueki N, Nakamura M, Mukumoto N, Nakamura A, Sakanaka K, Mizowaki T, Hiraoka M. Abdominal compression and respiratory motion as predictors of local recurrence in patients treated with stereotactic body radiation therapy for primary lung cancer. Int J Radiat Oncol Biol Phys. 2011;81(2):S608.
93. Wang L, Feigenberg S, Fan J, Jin L, Turaka A, Chen L, et al. Target repositional accuracy and PTV margin verification using three-dimensional cone-beam computed tomography (CBCT) in stereotactic body radiotherapy (SBRT) of lung cancers. J Appl Clin Med Phys. 2012;13(2):3708.
94. Josipovic M, Persson GF, Logadottir A, Smulders B, Westmann G, Bangsgaard JP. Translational and rotational intra- and inter-fractional errors in patient and target position during a short course of frameless stereotactic body radiotherapy. Acta Oncol. 2012;51(5):610–7.
95. Li W, Purdie TG, Taremi M, Fung S, Brade A, Cho BC, et al. Effect of immobilization and performance status on intrafraction motion for stereotactic lung radiotherapy: analysis of 133 patients. Int J Radiat Oncol Biol Phys. 2011;81(5):1568–75.
96. Nagata Y, Takayama K, Matsuo Y, Norihisa Y, Mizowaki T, Sakamoto T, et al. Clinical outcomes of a phase I/II study of 48 Gy of stereotactic body radiotherapy in 4 fractions for primary lung cancer using a stereotactic body frame. Int J Radiat Oncol Biol Phys. 2005;63(5):1427–31.
97. Onishi H, Araki T, Shirato H, Nagata Y, Hiraoka M, Gomi K, et al. Stereotactic hypofractionated high-dose irradiation for stage I non-small cell lung carcinoma: clinical outcomes in 245 subjects in a Japanese multiinstitutional study. Cancer. 2004;101(7):1623–31.

98. Dunlap NE, Larner JM, Read PW, Kozower BD, Lau CL, Sheng K, et al. Size matters: a comparison of T1 and T2 peripheral non-small-cell lung cancers treated with stereotactic body radiation therapy (SBRT). J Thorac Cardiovasc Surg. 2010;140(3):583–9.
99. Grills IS, Hope AJ, Guckenberger M, Kestin LL, Werner-Wasik M, Yan D, et al. A collaborative analysis of stereotactic lung radiotherapy outcomes for early-stage non-small-cell lung cancer using daily online cone-beam computed tomography image-guided radiotherapy. J Thorac Oncol. 2012;7(9):1382–93.
100. Rowe BP, Boffa DJ, Wilson LD, Kim AW, Detterbeck FC, Decker RH. Stereotactic body radiotherapy for central lung tumors. J Thorac Oncol. 2012;7(9):1394–9.
101. Barriger RB, Forquer JA, Brabham JG, Andolino DL, Shapiro RH, Henderson MA, et al. A dose-volume analysis of radiation pneumonitis in non-small cell lung cancer patients treated with stereotactic body radiation therapy. Int J Radiat Oncol Biol Phys. 2012;82(1):457–62.
102. Onishi H, Shirato H, Nagata Y, Hiraoka M, Fujino M, Gomi K, et al. Hypofractionated stereotactic radiotherapy (HypoFXSRT) for stage I non-small cell lung cancer: updated results of 257 patients in a Japanese multi-institutional study. J Thorac Oncol. 2007;2(7 Suppl 3):S94–100.
103. Dunlap NE, Cai J, Biedermann GB, Yang W, Benedict SH, Sheng K, et al. Chest wall volume receiving >30 Gy predicts risk of severe pain and/or rib fracture after lung stereotactic body radiotherapy. Int J Radiat Oncol Biol Phys. 2010;76(3):796–801.
104. Stephans KL, Djemil T, Tendulkar RD, Robinson CG, Reddy CA, Videtic GM. Prediction of chest wall toxicity from lung stereotactic body radiotherapy (SBRT). Int J Radiat Oncol Biol Phys. 2012;82(2):974–80.
105. Welsh J, Thomas J, Shah D, Allen PK, Wei X, Mitchell K, et al. Obesity increases the risk of chest wall pain from thoracic stereotactic body radiation therapy. Int J Radiat Oncol Biol Phys. 2011;81(1):91–6.
106. Hess KR, Varadhachary GR, Taylor SH, Wei W, Raber MN, Lenzi R, et al. Metastatic patterns in adenocarcinoma. Cancer. 2006;106(7):1624–33.
107. Prasad KR, Young RS, Burra P, Zheng SS, Mazzaferro V, Moon DB, et al. Summary of candidate selection and expanded criteria for liver transplantation for hepatocellular carcinoma: a review and consensus statement. Liver Transpl. 2011;17 Suppl 2:S81–9.
108. Mazzaferro V, Bhoori S, Sposito C, Bongini M, Langer M, Miceli R, et al. Milan criteria in liver transplantation for hepatocellular carcinoma: an evidence-based analysis of 15 years of experience. Liver Transpl. 2011;17 Suppl 2:S44–57.
109. Rusthoven KE, Kavanagh BD, Cardenes H, Stieber VW, Burri SH, Feigenberg SJ, et al. Multi-institutional phase I/II trial of stereotactic body radiation therapy for liver metastases. J Clin Oncol. 2009;27(10):1572–8.
110. Tiong L, Maddern GJ. Systematic review and meta-analysis of survival and disease recurrence after radiofrequency ablation for hepatocellular carcinoma. Br J Surg. 2011;98(9):1210–24.
111. Fong Y, Cohen AM, Fortner JG, Enker WE, Turnbull AD, Coit DG, et al. Liver resection for colorectal metastases. J Clin Oncol. 1997;15(3):938–46.
112. Berber E, Pelley R, Siperstein AE. Predictors of survival after radiofrequency thermal ablation of colorectal cancer metastases to the liver: a prospective study. J Clin Oncol. 2005;23(7):1358–64.
113. Steele Jr G, Bleday R, Mayer RJ, Lindblad A, Petrelli N, Weaver D. A prospective evaluation of hepatic resection for colorectal carcinoma metastases to the liver: Gastrointestinal Tumor Study Group Protocol 6584. J Clin Oncol. 1991;9(7):1105–12.
114. Wagner JS, Adson MA, Van Heerden JA, Adson MH, Ilstrup DM. The natural history of hepatic metastases from colorectal cancer. A comparison with resective treatment. Ann Surg. 1984;199(5):502–8.
115. Kelly RJ, Kemeny NE, Leonard GD. Current strategies using hepatic arterial infusion chemotherapy for the treatment of colorectal cancer. Clin Colorectal Cancer. 2005;5(3):166–74.
116. Salem R, Lewandowski RJ, Mulcahy MF, Riaz A, Ryu RK, Ibrahim S, et al. Radioembolization for hepatocellular carcinoma using Yttrium-90 microspheres: a comprehensive report of long-term outcomes. Gastroenterology. 2010;138(1):52–64.
117. Vogl TJ, Zangos S, Eichler K, Yakoub D, Nabil M. Colorectal liver metastases: regional chemotherapy via transarterial chemoembolization (TACE) and hepatic chemoperfusion: an update. Eur Radiol. 2007;17(4):1025–34.
118. Fowler KJ, Brown JJ, Narra VR. Magnetic resonance imaging of focal liver lesions: approach to imaging diagnosis. Hepatology. 2011;54(6):2227–37.
119. Kelsey CR, Schefter T, Nash SR, Russ P, Baron AE, Zeng C, et al. Retrospective clinicopathologic correlation of gross tumor size of hepatocellular carcinoma: implications for stereotactic body radiotherapy. Am J Clin Oncol. 2005;28(6):576–80.
120. Mendez Romero A, Wunderink W, Hussain SM, De Pooter JA, Heijmen BJ, Nowak PC, et al. Stereotactic body radiation therapy for primary and metastatic liver tumors: a single institution phase I-II study. Acta Oncol. 2006;45(7):831–7.
121. Balter JM, Dawson LA, Kazanjian S, McGinn C, Brock KK, Lawrence T, et al. Determination of ventilatory liver movement via radiographic evaluation of diaphragm position. Int J Radiat Oncol Biol Phys. 2001;51(1):267–70.
122. Davies SC, Hill AL, Holmes RB, Halliwell M, Jackson PC. Ultrasound quantitation of respiratory organ motion in the upper abdomen. Br J Radiol. 1994;67(803):1096–102.
123. Aruga T, Itami J, Aruga M, Nakajima K, Shibata K, Nojo T, et al. Target volume definition for upper abdominal irradiation using CT scans obtained during inhale and exhale phases. Int J Radiat Oncol Biol Phys. 2000;48(2):465–9.
124. Kirilova A, Lockwood G, Choi P, Bana N, Haider MA, Brock KK, et al. Three-dimensional motion of liver tumors using cine-magnetic resonance imaging. Int J Radiat Oncol Biol Phys. 2008;71(4):1189–95.
125. Heinzerling JH, Anderson JF, Papiez L, Boike T, Chien S, Zhang G, et al. Four-dimensional computed tomography scan analysis of tumor and organ motion at varying levels of abdominal compression during stereotactic treatment of lung and liver. Int J Radiat Oncol Biol Phys. 2008;70(5):1571–8.
126. Eccles CL, Patel R, Simeonov AK, Lockwood G, Haider M, Dawson LA. Comparison of liver tumor motion with and without abdominal compression using cine-magnetic resonance imaging. Int J Radiat Oncol Biol Phys. 2011;79(2):602–8.
127. Eccles CL, Dawson LA, Moseley JL, Brock KK. Interfraction liver shape variability and impact on GTV position during liver stereotactic radiotherapy using abdominal compression. Int J Radiat Oncol Biol Phys. 2011;80(3):938–46.
128. Baek HM, Chen JH, Nie K, Yu HJ, Bahri S, Mehta RS, et al. Predicting pathologic response to neoadjuvant chemotherapy in breast cancer by using MR imaging and quantitative 1H MR spectroscopy. Radiology. 2009;251(3):653–62.
129. Hoyer M, Roed H, Sengelov L, Traberg A, Ohlhuis L, Pedersen J, et al. Phase-II study on stereotactic radiotherapy of locally advanced pancreatic carcinoma. Radiother Oncol. 2005;76(1):48–53.
130. Tse RV, Hawkins M, Lockwood G, Kim JJ, Cummings B, Knox J, et al. Phase I study of individualized stereotactic body radiotherapy for hepatocellular carcinoma and intrahepatic cholangiocarcinoma. J Clin Oncol. 2008;26(4):657–64.
131. Cardenes HR, Price TR, Perkins SM, Maluccio M, Kwo P, Breen TE, et al. Phase I feasibility trial of stereotactic body radiation therapy for primary hepatocellular carcinoma. Clin Transl Oncol. 2010;12(3):218–25.

132. Andolino DL, Johnson CS, Maluccio M, Kwo P, Tector AJ, Zook J, et al. Stereotactic body radiotherapy for primary hepatocellular carcinoma. Int J Radiat Oncol Biol Phys. 2011;81(4):e447–53.
133. Swaminath A, Dawson LA. Emerging role of radiotherapy in the management of liver metastases. Cancer J. 2010;16(2):150–5.
134. Klein J, Dawson LA. Hepatocellular carcinoma radiation therapy: review of evidence and future opportunities. Int J Radiat Oncol Biol Phys. 2013;87:22–32.
135. Wulf J, Guckenberger M, Haedinger U, Oppitz U, Mueller G, Baier K, et al. Stereotactic radiotherapy of primary liver cancer and hepatic metastases. Acta Oncol. 2006;45(7):838–47.
136. Rule W, Timmerman R, Tong L, Abdulrahman R, Meyer J, Boike T, et al. Phase I dose-escalation study of stereotactic body radiotherapy in patients with hepatic metastases. Ann Surg Oncol. 2011;18(4):1081–7.
137. Chang DT, Swaminath A, Kozak M, Weintraub J, Koong AC, Kim J, et al. Stereotactic body radiotherapy for colorectal liver metastases: a pooled analysis. Cancer. 2011;117(17):4060–9.
138. Goodman KA, Wiegner EA, Maturen KE, Zhang Z, Mo Q, Yang G, Gibbs IC, Fisher GA, Koong AC. Dose-escalation study of single-fraction stereotactic body radiotherapy for liver malignancies. Int J Radiat Oncol Biol Phys. 2010;78(2):486–93. doi:10.1016/j.ijrobp.2009.08.020. Epub 2010 Mar 28.
139. Fajardo LF, Colby TV. Pathogenesis of veno-occlusive liver disease after radiation. Arch Pathol Lab Med. 1980;104(11):584–8.
140. Sempoux C, Horsmans Y, Geubel A, Fraikin J, Van Beers BE, Gigot JF, et al. Severe radiation-induced liver disease following localized radiation therapy for biliopancreatic carcinoma: activation of hepatic stellate cells as an early event. Hepatology. 1997;26(1):128–34.
141. Cheng AS, Chan HL, Leung WK, To KF, Go MY, Chan JY, et al. Expression of HBx and COX-2 in chronic hepatitis B, cirrhosis and hepatocellular carcinoma: implication of HBx in upregulation of COX-2. Mod Pathol. 2004;17(10):1169–79.
142. Lawrence TS, Robertson JM, Anscher MS, Jirtle RL, Ensminger WD, Fajardo LF. Hepatic toxicity resulting from cancer treatment. Int J Radiat Oncol Biol Phys. 1995;31(5):1237–48.
143. Emami B, Lyman J, Brown A, Coia L, Goitein M, Munzenrider JE, et al. Tolerance of normal tissue to therapeutic irradiation. Int J Radiat Oncol Biol Phys. 1991;21(1):109–22.
144. Dawson LA, Ten Haken RK. Partial volume tolerance of the liver to radiation. Semin Radiat Oncol. 2005;15(4):279–83.
145. Oettle H, Post S, Neuhaus P, Gellert K, Langrehr J, Ridwelski K, et al. Adjuvant chemotherapy with gemcitabine vs observation in patients undergoing curative-intent resection of pancreatic cancer: a randomized controlled trial. JAMA. 2007;297(3):267–77.
146. Regine WF, Winter KA, Abrams RA, Safran H, Hoffman JP, Konski A, et al. Fluorouracil vs gemcitabine chemotherapy before and after fluorouracil-based chemoradiation following resection of pancreatic adenocarcinoma: a randomized controlled trial. JAMA. 2008;299(9):1019–26.
147. Pisters PW, Wolff RA, Janjan NA, Cleary KR, Charnsangavej C, Crane CN, et al. Preoperative paclitaxel and concurrent rapid-fractionation radiation for resectable pancreatic adenocarcinoma: toxicities, histologic response rates, and event-free outcome. J Clin Oncol. 2002;20(10):2537–44.
148. Varadhachary GR, Wolff RA, Crane CH, Sun CC, Lee JE, Pisters PW, et al. Preoperative gemcitabine and cisplatin followed by gemcitabine-based chemoradiation for resectable adenocarcinoma of the pancreatic head. J Clin Oncol. 2008;26(21):3487–95.
149. Koong AC, Christofferson E, Le QT, Goodman KA, Ho A, Kuo T, et al. Phase II study to assess the efficacy of conventionally fractionated radiotherapy followed by a stereotactic radiosurgery boost in patients with locally advanced pancreatic cancer. Int J Radiat Oncol Biol Phys. 2005;63(2):320–3.
150. Polistina F, Costantin G, Casamassima F, Francescon P, Guglielmi R, Panizzoni G, et al. Unresectable locally advanced pancreatic cancer: a multimodal treatment using neoadjuvant chemoradiotherapy (gemcitabine plus stereotactic radiosurgery) and subsequent surgical exploration. Ann Surg Oncol. 2010;17(8):2092–101.
151. Mahadevan A, Jain S, Goldstein M, Miksad R, Pleskow D, Sawhney M, et al. Stereotactic body radiotherapy and gemcitabine for locally advanced pancreatic cancer. Int J Radiat Oncol Biol Phys. 2010;78(3):735–42.
152. Schellenberg D, Goodman KA, Lee F, Chang S, Kuo T, Ford JM, et al. Gemcitabine chemotherapy and single-fraction stereotactic body radiotherapy for locally advanced pancreatic cancer. Int J Radiat Oncol Biol Phys. 2008;72(3):678–86.
153. Chang DT, Schellenberg D, Shen J, Kim J, Goodman KA, Fisher GA, et al. Stereotactic radiotherapy for unresectable adenocarcinoma of the pancreas. Cancer. 2009;115(3):665–72.
154. Murphy JD, Christman-Skieller C, Kim J, Dieterich S, Chang DT, Koong AC. A dosimetric model of duodenal toxicity after stereotactic body radiotherapy for pancreatic cancer. Int J Radiat Oncol Biol Phys. 2010;78(5):1420–6.
155. Rwigema JC, Parikh SD, Heron DE, Howell M, Zeh H, Moser AJ, et al. Stereotactic body radiotherapy in the treatment of advanced adenocarcinoma of the pancreas. Am J Clin Oncol. 2011;34(1):63–9.
156. Van Laethem JL, Hammel P, Mornex F, Azria D, Van Tienhoven G, Vergauwe P, et al. Adjuvant gemcitabine alone versus gemcitabine-based chemoradiotherapy after curative resection for pancreatic cancer: a randomized EORTC-40013–22012/FFCD-9203/GERCOR phase II study. J Clin Oncol. 2010;28(29):4450–6.
157. Conroy T, Gavoille C, Samalin E, Ychou M, Ducreux M. The role of the FOLFIRINOX regimen for advanced pancreatic cancer. Curr Oncol Rep. 2013;15:182–9.
158. Conroy T, Mitry E. [Chemotherapy of metastatic pancreatic adenocarcinoma: challenges and encouraging results]. Bull Cancer. 2011;98(12):1439–46.